Biosensors and Bioelectronics 141 (2019) 111418

Contents lists available at ScienceDirect

Biosensors and Bioelectronics

journal homepage: www.elsevier.com/locate/bios

Advances in biosensors for the detection of ochratoxin A: Bio-receptors, nanomaterials, and their applications

Yasmin Alhamoud[a], Danting Yang[a,b,*], Samuel Selorm Fiati Kenston[a], Guozhen Liu[b], Linyang Liu[b], Haibo Zhou[c], Fatma Ahmed[a], Jinshun Zhao[a,**]

[a] Department of Preventative Medicine, Zhejiang Key Laboratory of Pathophysiology, Medical School of Ningbo University, 818 Fenghua Road, Ningbo, Zhejiang Province, 315211, People's Republic of China

[b] Graduate School of Biomedical Engineering, ARC Centre of Excellence in Nanoscale BioPhotonics (CNBP), Faculty of Engineering, The University of New South Wales, Sydney, Sydney, 2052, Australia

[c] Institute of Pharmaceutical Analysis and Guangdong Province Key Laboratory of Pharmacodynamic Constituents of Traditional Chinese Medicine & New Drug Research, College of Pharmacy, Jinan University, Guangzhou, 510632, China

ARTICLE INFO

Keywords:
Ochratoxin A
Bio-receptors
Nanomaterials
Biosensors
Applications

ABSTRACT

Ochratoxin A (OTA) is a class of mycotoxin mainly produced by the genera Aspergillus and Penicillium. OTA can cause various forms of kidney, liver and brain diseases in both humans and animals although trace amount of OTA is normally present in food. Therefore, development of fast and sensitive detection technique is essential for accurate diagnosis of OTA. Currently, the most commonly used detection methods are enzyme-linked immune sorbent assays (ELISA) and chromatographic techniques. These techniques are sensitive but time consuming, and require expensive equipment, highly trained operators, as well as extensive preparation steps. These drawbacks limit their wide application in OTA detection. On the contrary, biosensors hold a great potential for OTA detection at for both research and industry because they are less expensive, rapid, sensitive, specific, simple and portable. This paper aims to provide an extensive overview on biosensors for OTA detection by highlighting the main biosensing recognition elements for OTA, the most commonly used nanomaterials for fabricating the sensing interface, and their applications in different read-out types of biosensors. Current challenges and future perspectives are discussed as well.

1. Introduction

The expression "mycotoxin" is typically held for small compounds (roughly 300-700 Da), which are created both pre-and post-harvest as secondary metabolites by a few unique fungal species (Turner et al., 2015). Although around 400 basic mycotoxins have been recognized, only a few of them are viewed as the major and significant compounds of interest, such as ochratoxin, aflatoxin, deoxynivalenol, nivalenol, 3-acetyl-deoxynivalenol, 15-acetyl-deoxynivalenol, zearalenone, trichothecenes, and fumonisin. The above mycotoxins have negative impact on both animal and human health in food commodities, more frequently enhancing the risk of chronic diseases than food additives or pesticide residue (van Egmond et al., 2007). Hence their identification is a great scientific importance for the sake of animal and human health. Ochratoxin A (7-(L-β phenylalanyl carbonyl)-carboxyl-5-chloro-8 hydroxy-3,4-dihydro-3R-methyl-isocumarin, OTA), one key group of mycotoxins, is produced mainly by two genera: Aspergillus and Penicillium. It exists in daily food items such as coffee, cocoa, cereals, nuts, spices, eggs, meat, beer, wine, dairy and fruits (Fernández-Cruz et al., 2010; Iqbal et al., 2016; Yang et al., 2015a). Among the ochratoxin categories A, B, and C, OTA is the most abundant and harmful food contaminating mycotoxin (Ajeet et al., 2009; El Khoury and Atoui, 2010). It has been implicated as being nephrotoxic, hepatotoxic, neurotoxic, teratogenic, carcinogenic and immunotoxic to humans (El Khoury and Atoui, 2010; Zhang et al., 2015). Therefore, OTA was categorized in group 2B as possible human carcinogen by the International Agency for Research on Cancer (IARC) (1993). Regulatory limits of OTA level in foodstuffs are strictly laid down up to now. Take the European Union for example, the maximum concentration in cereals was set to 5 ppb, while 2 ppb and 5 ppb was set for wine (or grape juice)

* Corresponding author. Department of Preventative Medicine, Medical School of Ningbo University, 818 Fenghua Road, Ningbo, Zhejiang Province, 315211, People's Republic of China.

** Corresponding author.

E-mail addresses: yangdanting@nbu.edu.cn (D. Yang), zhaojinshun@nbu.edu.cn (J. Zhao).

https://doi.org/10.1016/j.bios.2019.111418
Received 26 March 2019; Received in revised form 4 June 2019; Accepted 4 June 2019
Available online 06 June 2019
0956-5663/

and to coffee products, respectively. In order to minimize the life-threatening risks caused by OTA and meet the regulatory limits for a variety of foodstuffs, various detection techniques of OTA have been developed (Ha, 2015).

Chromatographic methods such as high-performance liquid chromatography (HPLC) (Majdinasab et al., 2015), liquid chromatography (LC) assisted with mass spectrometry (MS) (Andrade and Lanças, 2017; Mariño-Repizo et al., 2015) or fluorescence detection (Savastano et al., 2016) have been developed. Gas chromatography (GC) coupled with MS (Olsson et al., 2002), capillary electrophoresis (Xiao et al., 2018), and thin layer chromatography (TLC) (Teixeira et al., 2011) are good options for OTA detection due to their sensitivity, selectivity and reliability. However, they are time-consuming, and require expensive equipment, highly trained operators, and huge amount of solvents. The conventional ELISA method, well known for its sensitivity, is used for OTA detection relying on precise antibodies recognizing OTA with high affinity and specificity (Zhang et al., 2011). Customary microwell plate indirect competitive ELISA products for the OTA detection can be acquired industrially, nonetheless, they are time and reagent devouring, and rely upon massive equipment (Novo et al., 2013). Lately, to improve assay sensitivity and construct effortless ELISA, nanotechnology combining with different read-out techniques such as fluorescence, colorimetry, and chemiluminescence has been connected to conventional ELISA for OTA detection (Wu et al., 2019; Liang et al., 2016; Pei et al., 2018; Shen et al., 2017; Sun et al., 2019), with a few issues such as high cost, long reaction time and tedious operations still existing. Hence, the biosensor-based detection strategy as rapid, easy, accurate, portable, and cheap tool is promising to rectify the challenges.

Recently, several comprehensive reviews regarding this subject have been published. For instance, Badie Bostan et al. (2017) summarized the recent advancements in OTA detection based on aptasensors and highlighted the advantages and disadvantages of different types of OTA aptasensors. Jiang et al. (2018) discussed the current progress and application of nanomaterial-based biosensors for OTA determination. Moreover, Goud et al. (2018) summed up the recent developments of nanomaterial-based electrochemical (EC) biosensors for mycotoxin detection highlighting the role of carbon and graphene metal nanoparticles (NPs) with different recognition elements. Each fantastic review provides single specific topic such as aptasensors, nanomaterial-based OTA biosensors, or EC biosensors for mycotoxin detection. To our knowledge, there is no review systematically and comprehensively introduces OTA biosensor involving bioreceptors, nanomaterials, and their applications in different read-out modes, which engage as three essential segments of biosensor. Therefore, in this review, we provide an extensive overview on the recent developments in these three aspects for OTA determination. Firstly, bioreceptors including conventional antibodies and their alternatives (nanobodies, peptides, molecularly imprinted polymers, aptamer and DNases) which can recognize OTA, are thoroughly discussed. Secondly, different types of nanomaterials (carbon nanomaterials, super paramagnetic particles, metal nanomaterials, quantum dots, up-conversion NPs, and metal-organic frameworks) for fabricating the sensing interfaces are demonstrated. Subsequently, advanced applications of different read-out modes (optics, electrochemistry, mass-sensitivity, and surface-enhanced Raman spectroscopy) for OTA sensing involving bioreceptors and nanomaterials are summarized. Finally, current challenges and prospects regarding OTA biosensors are investigated as well.

2. Types of bio-receptors (recognition elements)

The bio-receptor, or also called the recognition element is the most crucial aspect of biosensors which make the sensitive and selective analysis possible. In this section, different types of bio-receptors for OTA detection including antibody/nanobody (Ab/Nb), peptides, molecularly imprinted polymer (MIP), and aptamer/DNAzyme, are introduced.

2.1. Antibody and nanobody (VHHs antibody)

Antibodies (Abs) in our immune system help the body to defend against intruding substances and organisms, including IgA, IgD, IgE, IgG, IgM, and IgY (avian) produced by specialized cells of the immune system (Meulenberg, 2012). As the gold standard recognition elements, varieties of antibodies including polyclonal antibodies (pAbs), monoclonal antibodies (mAbs), or chemically labeled enzymes such as horseradish peroxidase (HRP) and alkaline phosphatase, have been used in biosensors of OTA and other mycotoxins because of their unique properties and specificities (Karczmarczyk et al., 2017a; Lu et al., 2016; Malvano et al., 2016b; Regiart et al., 2018; Solanki et al., 2017; Yu et al., 2018a; Zhang et al., 2016b). However, the acquisition process of high-quality antibodies is usually time-consuming, expensive, and depends on immunization with the risk of poor solubility. The chemical conjugation of enzymes to antibodies may also lead to unstable and randomly cross-linked molecules and further provide false results.

To overcome the aforementioned issues, various types of genetically engineered antibodies such as recombinant antibody fragments Fab (antigen-binding fragment), scFv (single chain variable fragment), and single domain antibody (sdAb), have been investigated for biosensor fabrication. The sdAbs, also called as VHHs antibodies or nanobodies (Nbs), are derived from the variable region of heavy chain Abs existing in members of the Camelidae such as llamas, dromedaries, and camels, and VNAR fragments for cartilaginous fishes (De Meyer et al., 2014; De Groof et al., 2019). Nbs possess distinct properties such as low toxicity, higher solubility, and easier genetic editing with higher yield and refolding capacity (de Marco, 2011; Könning et al., 2017; Muyldermans, 2013; Steeland et al., 2016). They have comparable or greater sensitivity and affinity as well as superior physicochemical stability when comparing with Fab and scFv which are more susceptible to aggregate and have lower affinity for their target, along with better cleft-like epitopes than conventional Abs for mycotoxin detection (Holliger and Hudson, 2005). The Nbs developed by Liu et al. (2014) from an alpaca derived VHH library (Fig. 1A) are widely used for OTA detection both in phage display mediated immuno-polymerase chain reaction (PCR) and indirect competitive ELISA for OTA detection (Liu et al., 2017b). Recently, a polyvinylidene fluoride (PVDF) membrane-based dot immunoassay using a nanobody-alkaline phosphatase (Nb-AP) fusion protein for one-step, qualitative, and visual detection of OTA in cereals has been considered as a tremendous success (Fig. 1B), of which the cut-off limit was assessed by naked eye with a LOD of 0.3125 ng/mL in 6 min (Tang et al., 2018b). However, it is still very challenging to select the desirable Nbs which will bind to the small molecule epitopes from the phage display Nbs repertoire, limiting extensive applications of Nbs in mycotoxin.

2.2. Peptides

Peptides are formed by natural or synthetic short polymers of amino acids that are linked by peptide bonds with shorter lengths than those of proteins. They share the same chemical structure such as specific sequence with proteins and exhibit high stability, easy modification, and large chemical versatility, which makes them possible substitute for antibodies and the simplest bio-receptor for binding of some small molecules to improve the analytical performance of biosensors (Liu et al., 2015; Soleri et al., 2015). Specific peptide ligands of OTA used for analysis are available at a relatively low cost with the help of successful computational modeling program (Giraudi et al., 2015; Tozzi et al., 2002). In addition, phage-displayed peptides such as OTA mimotope, can be constructed from second-generation peptide library with higher binding affinities to targets (He et al., 2013) (Fig. 1 C) and used for ELISA based detection for OTA (Zou et al., 2016). HRP conjugated anti-M13 Abs phage displayed mimotope peptide of OTA used as a mimic of conventional competing antigen can help achieve lower LOD of 2.04 fg/mL in an EC immunosensor for OTA detection (Hou et al., 2018) (Fig. 1

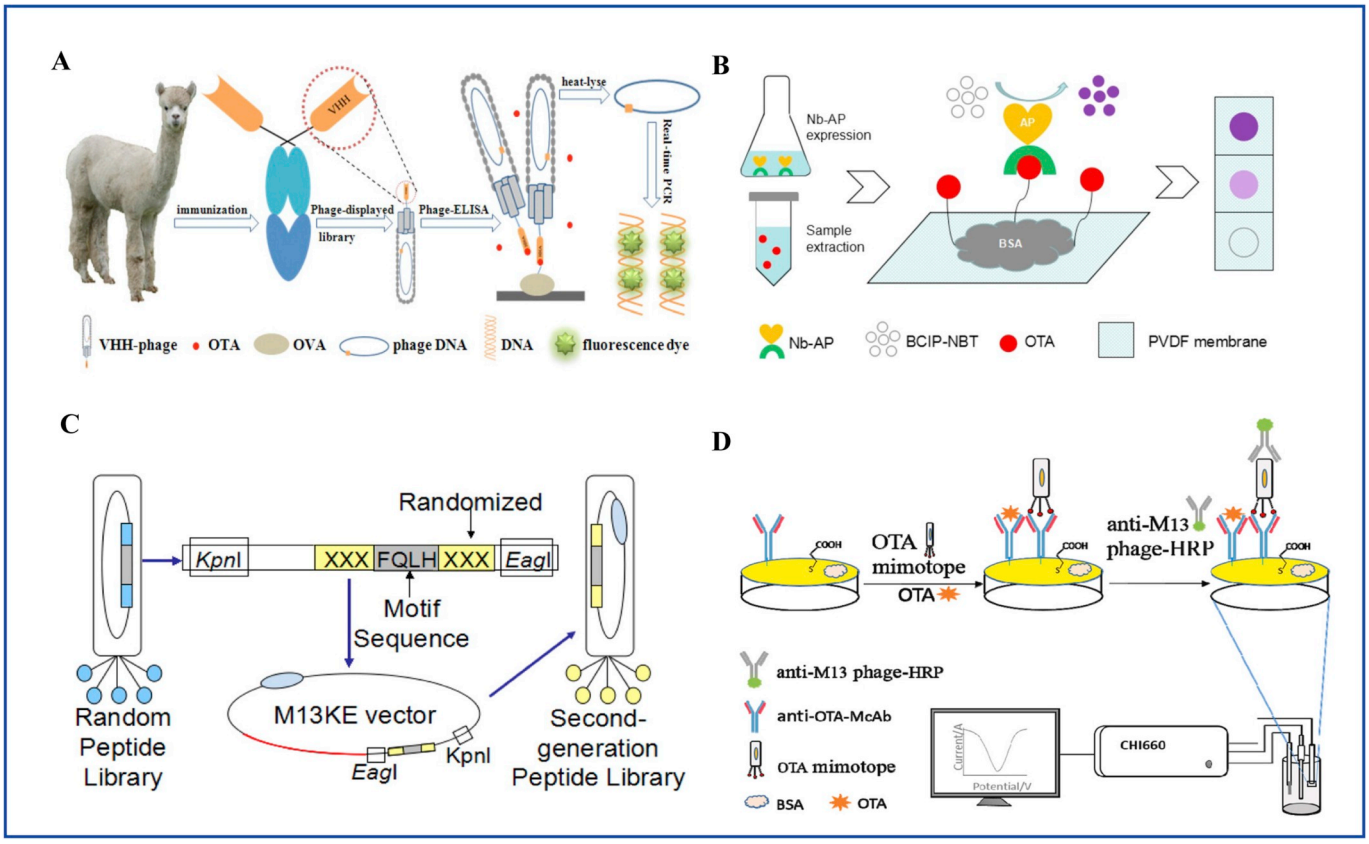

Fig. 1. Schematic of (A) VHHs antibody (Nanobody) developed from alpaca derived VHH library for OTA detection; (B) Nb-AP based immunoassay for visual detection of OTA in cereals; (C) Phage-displayed peptides produced form second-generation peptide library; (D) OTA minotope peptide used for forming an electrochemical immunosensor. The figures are reproduced from Ref (Liu et al., 2014; Tang et al., 2018b; He et al., 2013; Hou et al., 2018).

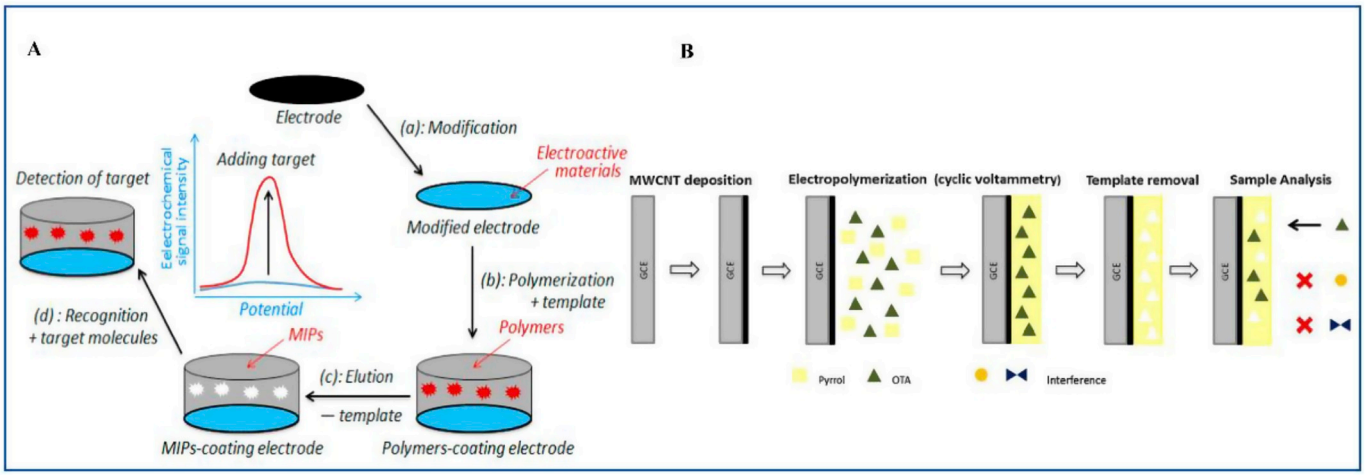

Fig. 2. Schematic of (A) Principle of fabrication, recognition, and detection based on MIPs-based electrochemical biosensors; (B) MIPs-based E-DNA biosensing. The figures are reproduced from Ref (Gui et al., 2018) and Ref (Pacheco et al., 2015), respectively.

D). Except for the phage display peptides, chemical synthesized small peptides (12 amino acids) also allowed the specific recognition of OTA. For instance, an amperometric and luminescence bioassay based on the peptide NFO_4 was able to finish the OTA detection in 40 min (Tria et al., 2016). However, only a few peptides have been successfully used as recognition elements of OTA because the design of new peptide receptors with high affinities is challenging due to the limited understanding of interactions involved in the molecular recognition.

2.3. Molecularly imprinted polymer (MIP)

Molecularly imprinted polymer (MIP), is the end-product of the molecular imprinting process when the template molecule (also known as target compound) is removed from a polymer. Non-covalent approach which relies on the relatively weak non-covalent interactions between the template molecule and selected monomer before polymerization, is probably the most often used strategy to form MIP (Zamora-Gálvez et al., 2017). Specific binding cavities with shape and functional groups complementary to the template are created within

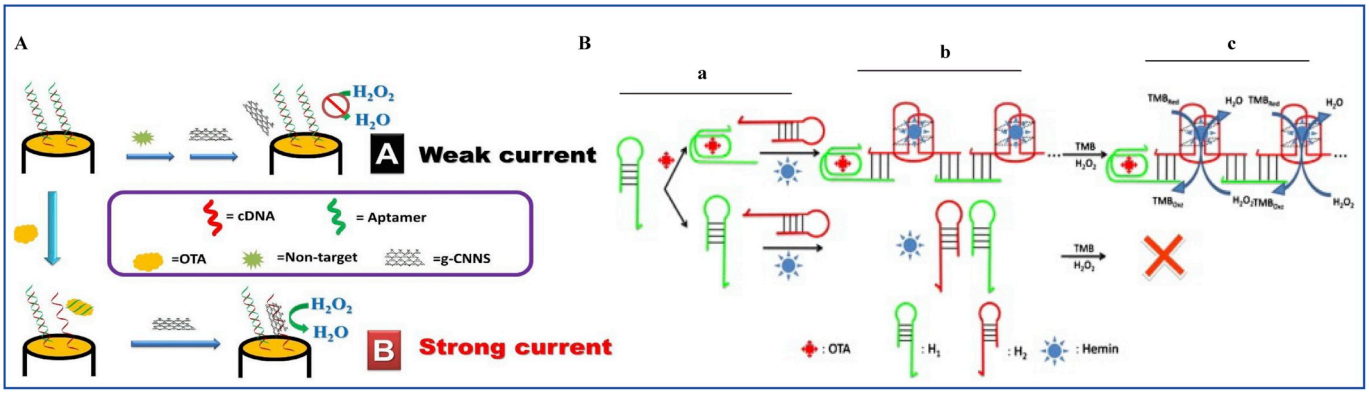

Fig. 3. Schematic of (A) Sensing mechanism of an OTA aptasensor; (B) OTA induced HCR process. H_1: contained aptamer, H_2 contained DNAzyme (a-formation of OTA aptamer in the presence of Ca^{2+}. (b-formation of G-quadruplex/hemin HRP-mimicking DNAzyme complexes in the presence of K^+. (c-catalyze $H_2O_2$by DNAzyme to oxidize TMB and produce colored products. The figures are reproduced from Ref (Zhu et al., 2018) and Ref (Wang et al., 2015a), respectively.

the polymer matrix (Ashley et al., 2017), which endows MIPs with high selectivity and ability to mimic natural recognition entities like antibodies and biological receptors (Poma et al., 2010; Yan et al., 2007). MIPs have been used as an efficient and powerful technique as SPE sorbent (MIP-SPE) for sample clean-up and pre-concentration of OTA (Cao et al., 2013), with the potential of being recognition elements for the extraction and analysis of OTA from food samples. They also have excellent mechanical robustness as well as strong resistance to elevated temperatures and pressures (Holthoff and Bright, 2007; Piletsky et al., 2006), making them suitable for biosensor construction. Although MIP-based EC, quartz crystal microbalance (QCM), and optical biosensors (Cieplak and Kutner, 2016) were investigated, most of the studies focused on MIP-based EC biosensors (ECBSs) for diverse target molecule detections in different fields, employing MIPs as specific recognition elements and smart devices as EC signal outputs shown in Fig. 2 A (Gu et al., 2016; Huang et al., 2017; Liu et al., 2017a; Ma et al., 2017; Silva et al., 2016; You et al., 2018; Gui et al., 2018) because of their prevalence for selective and sensitive sensing of targets. For example, in a sensitive and selective MIP-based ECBS for OTA detection in beer and wine developed by Pacheco et al. (2015) shown in Fig. 2B, the imprinted polypyrrole (PPy) film served as the selective recognition element of OTA and was first prepared by electropolymerization of pyrrole with OTA as a template molecule. The EC oxidation of OTA after the removal of template was then investigated by cyclic voltammetry (CV) and differential pulse voltammetry (DPV) to achieve the detection of OTA.

Introduction of surface chemistry alone or in combination with metal NPs, or magnetic NPs (MNPs) into molecular imprinting strategy can provide MIPs with higher binding capacities, faster binding kinetics, and easier coupling to the transducer surface than the traditional MIPs, which leads to a new perspective of MIPs for sensing purposes (Shanshan Wang, 2012; Turan and Şahin, 2016). For instance, when silver NPs (AgNPs)/a polyoxometalate ($H_3PW_{12}O_{40}$, POM)/reduced graphene oxide (rGO) nanocomposites were introduced to a MIP-voltammetric sensor toward OTA detection, an ultralow LOD of 0.16 pM was realized (Yola et al., 2016). Biocompatible MNPs-MIPs biosensors showed a fast and large adsorption capacity and high selectivity toward OTA (Turan and Şahin, 2016), with a good recovery in the spiked grape juice samples ranging from 97.1% to 97.4%. Notwithstanding the limited current available commercial and laboratory MIPs products and their low selectivity and binding affinity, the best MIPs performances with no specific methods are required for more investigation. Moreover, MIPs are not selective enough in the aqueous environment to compete with natural bio-receptors such as antibodies (Ashley et al., 2017).

2.4. Aptamer and DNAzymes

Aptamers are oligonucleotides (single stranded DNA (ssDNA) or RNA) containing 10-50 variable bases that can bind to a broad range of target analytes with great affinities (Cho et al., 2009; Wang et al., 2015c). The process of selecting a particular molecular sequence for aptamers synthesis is known as the systematic evolution of ligands by exponential enrichment (SELEX), which engages numerous cycles of selection and amplification of an oligonucleotide from a large library with different sequences. Upon incubation with specific target molecules and partitioning of the binding from non-binding molecules, selected oligonucleotides were amplified to create a new mixture comprising nucleic acid molecules with higher affinity towards the target (Mishra et al., 2018). Aptamers have been widely used as bio-receptor for numerous molecule analytes such as cells (Wang et al., 2017a), peptides (Ma et al., 2016), proteins (Tang et al., 2018a), ions (Wu et al., 2018a), amino acid (Yuan et al., 2018), bacteria (Dinshaw et al., 2017), and antibiotics (Yazdian robati et al., 2016).

Biosensors using aptamers as bio-recognition elements, also known as aptasensors, were first described in 1996 and have been applied in various toxins detection, especially for mycotoxin (Pfeiffer and Mayer, 2016; Niazi et al., 2018; Ren et al., 2017; Xiao et al., 2018; Yang et al., 2017). The first aptamer of OTA was isolated by Cruz-Agado and Penner in 2008 by employing the SELEX process (Cruz-Aguado and Penner, 2008). The OTA aptasensors are mainly based on label-free aptasensors adopting the natural target and bioreceptors without any modification and allow real-time study of biomolecular interactions with faster analysis (Cheng et al., 2012; Chauhan et al., 2016; Yin et al., 2017). In addition, they are less expensive because the hectic steps involved in labeling and challenging reactions are avoided. In Fig. 3A, the bioreceptor was firstly immobilized onto the transducer surface and incubated with the target directly. The analysis is then accomplished by studying the change in electrical or physical properties of the analytes, which entirely depended on the affinity of interaction between the analytes and their receptors (Zhu et al., 2018). Easy modification of aptamers helped control the orientation of immobilized aptamer (Witt et al., 2015). Being animal-free and stable in high temperature, high affinity and selectivity coupled with cost-effective production, make aptamers a tremendous alternative to antibodies or other bio-receptors in very complex matrices. Although lots of new aptasensors have been reported for targeting OTA, it is still concerned that the complex architectures with costly amplification procedures greatly impede their commercial boost. Aptasensing of small molecules is also time-consuming and produces non-specific interactions, compromising their wide applications.

Recently, DNAzymes (deoxyribozyme) as bio-receptor have emerged into aptamer-based OTA biosensor to increase the sensitivity.

Table 1
Comparative study of the properties of the bioreceptors (Bazin et al., 2017; Groff et al., 2015; Van Heeke et al. 2017; Liu et al., 2015; Zamora-Gálvez et al., 2017; Van Audenhove and Gettemans, 2016).

	Antibody	Nanobody	**Aptamer**	Peptide	MIP
Stability	Poor stability (susceptible to pH, salt, temperature) Sensitive to sample matrix effects	High stability	High stability Long shelf life at ambient temperature	Strong stability in comparison with antibody	High stability and resistance Long shelf life
Immobilization onto solid surface	Difficult on a hydrophobic solid surface Random inefficiency Complexed and time-consuming	Easy	Easy	Easy	Easy
Size and structural complexity	Large (~150-170 kDa) Multimeric, multi-domain with complex tertiary and quaternary structures	Small size(~15kDa) Monomeric structure	Small size (~12-30 kDa) 30~80 nucleotides in length	Small molecular weight (< 15 kDa)	Depend on the imprinted analyte
Production considerations (ease, speed, cost)	Difficult Several months to complete High cost	Largely automated Approximately two to eight weeks to produce Cost-efficient compared with antibody	Easy and rapid automated Economical for use in scale	Easy and rapid automated A few weeks Cost-efficient compared with antibody	Easy to synthesize and handle Quicker compared with antibody Low fabrication cost
Modification	Hardly engineered	Easily engineered	Easily engineered	Easily engineered	Easily engineered
Manufacturing and Development Process	In-vivo production Difficult to expose different epitopes of the same target for selection Difficult to obtain against non-immunogenic targets	In-vitro production Can be engineered to improve epitope recognition specificity Rapid selection in plant, prokaryotic, yeast, mammalian or insect cells Possible to obtain against non-immunogenic target	In-vitro production Able to expose different epitopes of the same target for selection Able to obtain against non-immunogenic target Improved batch-to-batch consistency	In-vitro production Able to obtain against non-immunogenic target	In-vitro production Able to obtain for diverse analytes
Specificity and selectivity	High specificity and affinity	High specificity and affinity	High specificity and affinity	High specificity High affinity but less than antibody	Small binding capacity High specificity Lower selectivity than antibody

DNAzymes are catalytic enzymes based on DNA (Mahdiannasser and Karami, 2018) and was first used as DNA artificial nucleic acids in 1994 (Breaker and Joyce, 1994). Apart from the high catalytic activity, they also exhibit high specificity for cofactors, excellent stability, low cost, and easy synthesis and modification (Zhao et al., 2015a). The combination of high selectivity of aptamer with the peroxidase-mimicking property of DNAzyme increases the sensitivity for OTA detection (Yang et al., 2013a). For instance, low LOD of 0.01 nM could be achieved in an HCR amplification based DNAzyme-aptasensor developed by Wang et al. (2015a) as shown in Fig. 3B. However, the microtiter plate readers cannot maintain the reaction solution at a constant temperature resulting in the fluctuation of the signals, which will affect the DNAzyme activity dramatically.

A comparative study of different bioreceptors with different properties are listed in Table 1 as follows for a clearer understanding.

3. Nanomaterials

Nanomaterials with excellent properties such as large surface area, enhanced surface reactivity due to the quantum confinement effects, good electrical conductivity and magnetic properties (Kaittanis et al., 2010; Nath et al., 2008) have been widely used for biosensing applications (Rai et al., 2015). In this section, different types of nanomaterials including carbon nanomaterials, super paramagnetic particles, metal nanomaterials, quantum dots, upconversion NPs, and metal-organic frameworks, together with the advantages, disadvantages, and functions in biosensing are introduced.

3.1. Carbon nanomaterials

Carbon nanomaterials (CNMs), especially carbon nanotubes (CNTs) and graphene (Gr), have unique electrical, optical, thermal, mechanical and chemical properties, which make them ideal for biosensors. These great properties do depend on not only their functional atomic structures but also the interactions with other materials, such as gold NPs (AuNPs), SiO_2 and chitosan. CNMs can quench the fluorescence of the absorbed dyes, thus, it is possible to build variety of biosensors especially in combination with aptamer technology (Hermann and Patel, 2000). CNTs including single-walled carbon nanotube (SWNTs) and multi-walled carbon nanotubes (MWNTs) are believed to hold huge potential in analytical field (Guo et al., 2011; Norouzi et al., 2015). Graphene (Gr), another form of CNMs, has similar electrical, optical, and thermal properties as CNTs but in two-dimensional atomic sheet structure. Its structure contributes to versatile electronic characteristics, and avoids the problems associated with metal alloy NPs and CNTs (Cha et al., 2013). Therefore, Gr along with its composites such as graphene oxide (GO) and reduced graphene oxide (rGO) exhibit potential applicability in EC biosensors (Kuila et al., 2011; Filip and Tkac, 2014). Their morphology and relation are shown in Fig. 4 A. Although Gr is regarded as a perfect material for the construction of EC sensors for it has higher electrical conductivity than GO and rGO (Wang et al., 2016f), rGO is chosen more often for EC biosensors because its larger surface area, easier and more effective fabrication on the sensing interface, and higher stability on the immobilized NPs electrocatalytic compounds (Gupta et al., 2017; Qian et al., 2014; Rowley-Neale et al., 2018). Recently, graphene quantum dots (GQDs) (Fig. 4 B), a class of layered graphene sheets with lateral dimension smaller than 100 nm, have drawn increased attention due to their desirable photophysical, physicochemical low cytotoxicity, and high-water solubility properties (Zhao et al., 2016; Mondal et al., 2015). They are more promising than the traditional semiconductor QDs, and therefore they could be designed as a good fluorescent probe for biosensing with their fluorescent signal easily switched on and off through controlling the disaggregation/aggregation state of GQDs (Wang et al., 2017c; Tian et al., 2018).

3.2. Super paramagnetic particles

In order to minimize matrix effects and obtain appropriate recovery of the targets from real samples, sample pre-treatment step is quite crucial in biosensing procedures. Different sample preparation procedures such as immunoaffinity columns (IACs) (Zhao et al., 2014), liquid-liquid extraction (LLE/LLME), pressurized liquid extraction (PLE) (Zinedine et al., 2010), dispersive liquid-liquid microextraction (DLLME) (Lai et al., 2014), and solid phase extraction (SPE/SPME) (Zhu et al., 2016), have been developed. However, some of them are tedious and time-consuming, or lack of selectivity. Super paramagnetic particles such as magnetic beads (MBs) ($< 100\,\mu m$) and magnetic NPs (MNPs) (< 100 nm) have been increasingly used to separate the OTA from the complex sample matrices. They commonly composed of magnetic elements such as iron, nickel, cobalt and their oxides, which can be magnetized or integrated into the transducer materials when they are subjected to an external magnetic field (Wang et al., 2017d). Typically for biosensor applications, they are conjugated with antibodies or aptamers with the capability to quickly and efficiently identify and capture the analytes in crude samples. Moreover, they are considered as signal amplification methods to achieve picogram level detection in an effective and recyclable way for OTA pretreatment and detection (Fig. 4C) (Fernández-Baldo et al., 2010; Shao et al., 2018). The utilization of super paramagnetic particles reduces the amount of organic solvents needed in the sample preparation, shortens the separation time, simplifies the pretreatment process of the trace detection, and provides signal amplification for detection.

3.3. Metal nanomaterials

Metal nanomaterials (MNs) including metal oxide and noble metal, are perfect for improving the selectivity and sensitivity of biosensors due to their physical, chemical and optoelectronic properties (Burris and Stewart, 2012). MNs as modification components of electrodes, label carriers, and/or signal enhancers, can be integrated into ECBSs to increase the EC signals and obtain a lower LOD (George et al., 2018; Wang et al., 2018b). Metal oxide nanostructures (MONPs) (e.g IrO_2 NPs, CeO_2 NPs in sole gel, ZnO NPs, SiO_2NPs, TiO_2 NPs) are considered as revolutionary nanomaterials for the immobilization of biomolecules in biosensors due to their enhanced biological activities, great orientation and good conformation (Willander et al., 2014; Sharma et al., 2015). The employment of IrO_2 NPs could help to achieve ultrasensitive determination of OTA with LOD of 5.65 pg/mL (Rivas et al., 2015) for instance.

Noble metal NPs, normally AuNPs, AgNPs, and copper NPs (Cu NPs), are among the most extensively studied nanomaterials due to their unique optical, thermal, and electronic properties. They also possess excellent compatibility with biomolecules, strong chemical stability as well as ease of synthesis ability. Nobel metal NPs play a crucial role in the development of advanced biosensors to fulfill more specialized and sensitive biomolecular diagnostics (Doria et al., 2012). For instance, AuNPs provide excellent platforms for colorimetric biosensors as they can be easily functionalized and display different colors (from pink to violet and pale blue) depending on size, shape, and state of aggregation as shown in Fig. 5A (Aldewachi et al., 2018). Moreover, well dispersed AuNPs showed better fluorescence quenching effect than the aggregated ones, have been widely used to develop a sensitive fluorescence sensor for OTA analysis (Lv et al., 2017c).

3.4. Quantum dots

Quantum dots (QDs) are semiconductor NPs with unique electronic and optical properties. The diameter of QDs ranges between 1-20 nm and one NP contains about 100 to100,000 atoms. QDs have excellent properties such as high quantum yield, high molar extinction coefficients, broad absorption spectra, narrow and symmetric emission bands

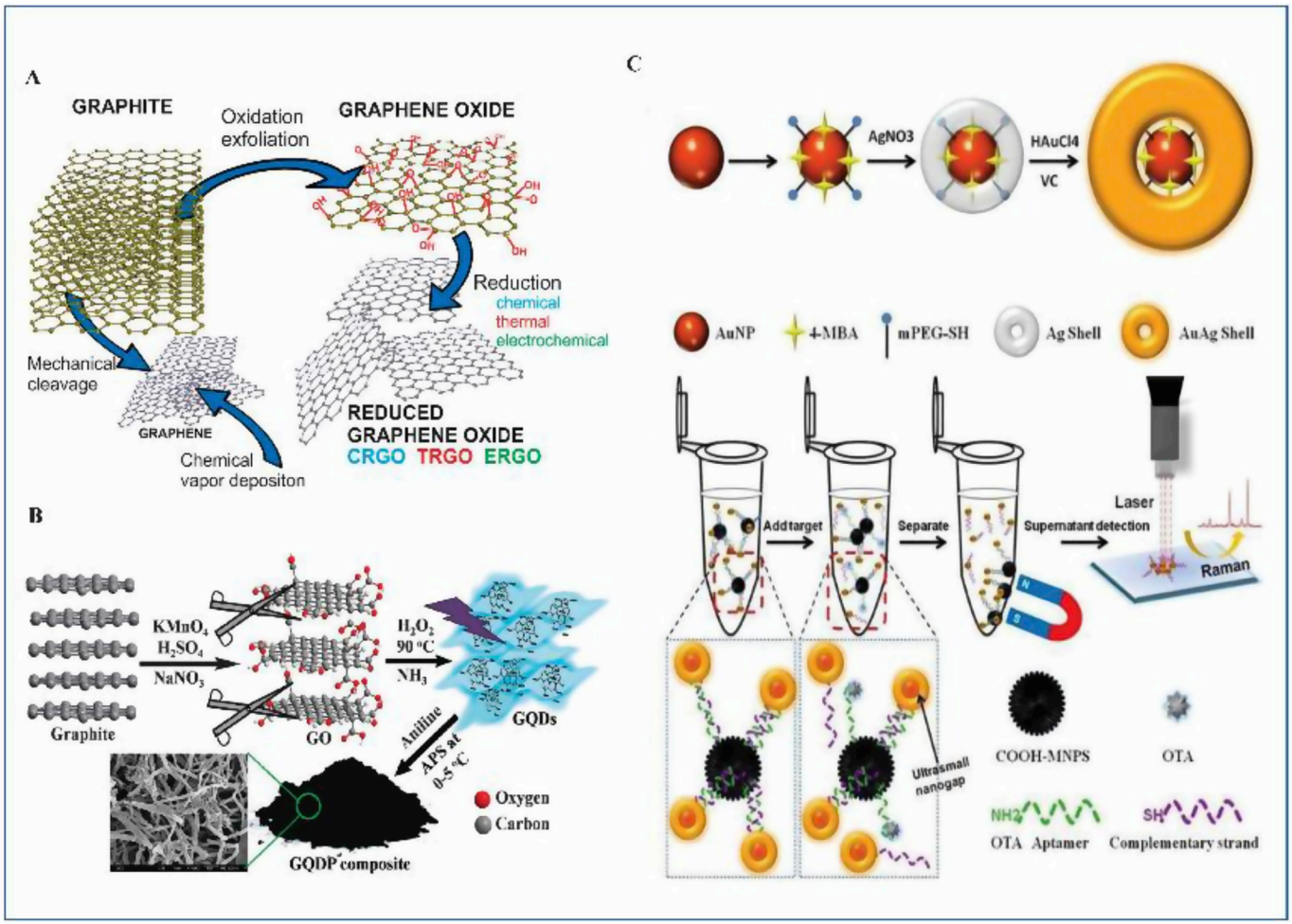

Fig. 4. Schematic of (A) structures of graphene, GO, and rGO; (B) GQDs; (C) how MNPs was used in pretreatment and detection cycle. The figures are reproduced from Ref (Filip and Tkac, 2014), Ref (Mondal et al., 2015), and Ref (Shao et al., 2018), respectively.

(30-50 nm) as well as high resistance to photo-bleaching and chemical degradation (Xu et al., 2016). Generally, QDs are composed of compounds formed by Zn and Cd with Te and Se (Gill et al., 2008) and have been employed in biosensing field for OTA detection as fluorescence labels (Yao et al., 2017) or EC labels (Tong et al., 2012). In many cases, they are usually conjugated to highly specific biomolecules like antibodies (Mahdi et al., 2016), and aptamers (Chu et al., 2016, Fig. 5B) to improve the selectivity of the assay.

3.5. Other nanomaterials

Upconversion NPs (UCNPs) are a new generation of fluorescent nanomaterials owing to their unique physicochemical characteristics, including high resistance to photobleaching and photoblinking, long lifetime, and sharp emission bands. Low toxicity, high color purity, multicolor tunable properties, high chemical stability, and low background fluorescence make them ideal for use in the construction of fluorescence-based sensors tagged with aptamers for biosensing of various target compounds (Ge et al., 2017). One example of UCNPs integrating with aptamer is shown in Fig. 5C (Wu et al., 2018a). Metal-organic frameworks (MOFs) is a novel type of highly porous crystalline material, constructed by the self-assembly of inorganic metal-containing nodes and organic ligands via strong coordination bonds. MOFs possess diverse sensing properties such as high specific surface areas, tunable pore sizes and exposed active sites as well as simple synthesis, making them promising candidates as colorimetric, fluorescent, and electrochemical signal reporters used in sensing applications. In addition, the exceedingly ordered pores in MOFs make them ideal immobilization matrixes to encapsulate a serial of functional substances (Qiu et al., 2019). The principle of MOFs engaging in an EC biosensor for OTA is illustrated as Fig. 5D.

The parameters including properties, disadvantages, and functions of the major nanomaterials in OTA biosensors listed above were summed up in Table 2 for a clearer understanding.

4. Applications of different read-out biosensors integrated with bioreceptors and nanomaterials

The integration of bioreceptors, nanomaterials, and different read-out techniques is capable to accomplish the rapid, sensitive, and multiplexed detection of OTA. In this section, the advanced applications of different read-out biosensors including optical, EC, mass-sensitivity, and surface-enhanced Raman spectroscopy biosensors, integrated with the aforementioned bio-receptors and nanomaterials, are discussed.

4.1. Optical biosensors

Optical methods, such as colorimetric, fluorescent, chemiluminescent and surface plasmon resonant strategies, are good techniques for OTA detection due to their simplicity, rapidity, reliability, and high sensitivity.

4.1.1. Colorimetric biosensors

The colorimetric detection principle utilizes a specific analyte to

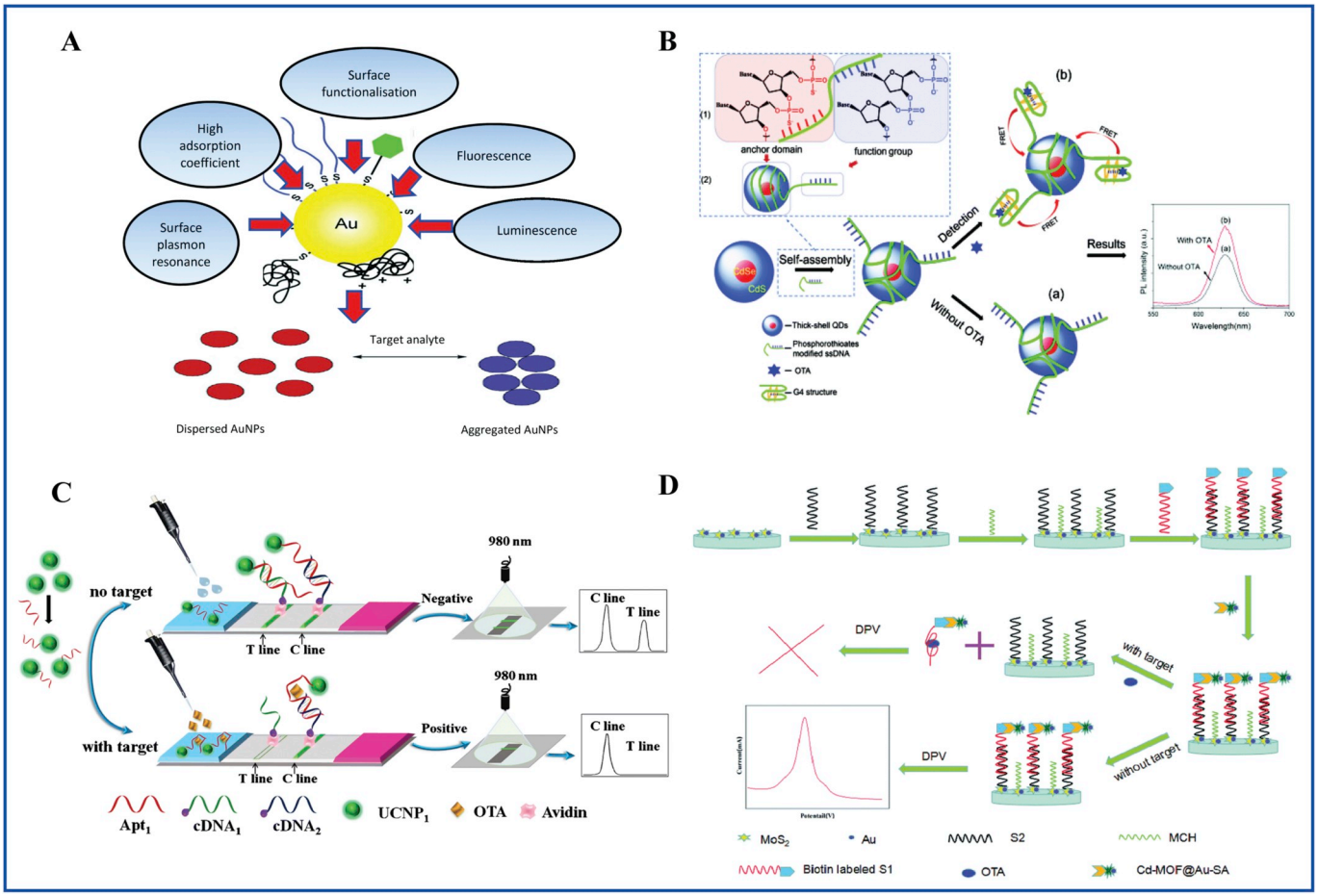

Fig. 5. Schematic of the principle of (A) AuNPs; (B) QDs; (C) UCNPs; (D) MOFs in OTA detection. The figures are reproduced from Ref (Aldewachi et al., 2018), Ref (Chu et al., 2016), Ref (Wu et al., 2018a), and Ref (Li et al., 2018), respectively.

induce the adsorption changes of nanomaterials, resulting in color changes that can be easily interpreted by the naked eyes (Terra et al., 2017). The simplicity, suitability for real-time detection, low amenability, as well as the easy preparation steps make the colorimetric strategy superior to many other detection methods (Hung et al., 2010). Aptamers in combination with AuNPs are commonly utilized in colorimetric detection of OTA (Xu et al., 2016). Yin et al. (2017) developed an aptamer-based colorimetric method for OTA detection in fortified white grape wine. In the study, a 36-mer aptamer was applied because of higher recognition than that of longer aptamers. Without OTA, the aptamer adsorbed on the surface of AuNPs prevented the aggregation of AuNPs with an original red color. When the OTA was added, the aptamer would bind to OTA and leave the AuNPs aggregated in solution exhibiting a blue color. The aptamer-based sensor exhibited a LOD of 20 ng/mL and excellent selectivity towards OTA as well as reliability for real samples with the good recoveries of 100.80 - 112.50%. Synergistic peroxidase-like Au@Fe_3O_4NPs (Wang et al., 2016b), enzyme-encapsulated liposomes (Lin et al., 2018) were also used to achieve an ultra-sensitive aptasensor for detection of OTA. For example, Lin et al. (2018) designed a dumbbell-shaped probe, including MBs, double-stranded DNA (dsDNA), and the enzyme-encapsulated liposome-based OTA biosensor which is shown in Fig. 6A. The dsDNA formed by the hybridization between OTA aptamer and its complementary probe, was used to contact with the MBs and the enzyme-encapsulated liposome. In the presence of OTA, the aptamer preferred to combine with OTA to form G-quadruplex, resulting in the release of the detection probe and the enzyme-encapsulated liposome. When the liposome was lysed by adding mixed solution of 3,3′, 5,5′-tetramethylbenzidine (TMB) and H_2O_2, HRP were released and catalyzed H_2O_2-mediated oxidation of TMB resulting in the color change from colorless to blue with the OTA concentration varying from 0.05 to 2.0 ng/mL. The LOD of 0.023 ng/mL and good recovery of 98.5%-106.1% indicated that the method was reliable for the analysis of real samples. Another promising application is the combination of colorimetric method with lateral flow assay (LFA) which is robust, less expensive and user-friendly for detection of OTA. Wu et al. (2018b) reported a novel competitive LFA employing aptamer functionalized UCNP (NaYF4:Yb, Er) as a reporter probe for the detection of OTA. As shown in Fig. 5C, visible green fluorescence signal on T line was observed under the excitation of 980 nm laser with the absence of OTA in the samples. When OTA was introduced, a diminished green fluorescence signal was observed on T line. Good analytical performance was observed with LOD of 1.86 ng/mL in spiked wheat and beer samples. This assay can be performed within 15 min and showed no serious cross-sensitivity to potentially interfering species, demonstrating good accuracy and repeatability.

4.1.2. *Surface plasmon resonance-based biosensors*

Surface plasmon resonance (SPR) based sensor is an affinity optical sensor providing a real-time and highly sensitive response on the binding of molecules of interest to the sensor's surface without the use of molecular labels. Therefore, it has attracted attention due to the high specific detection of target analytes in complex matrices (Mahmoudpour et al., 2019). In brief, SPR characterizes surface refractive index change which is very sensitive to analytes contacting with the sensor surface and amount of biomolecular layer (dielectric medium) immobilized on the sensor surface (Mohammadzadeh-Asl et al., 2018). In a SPR assay, direct and indirect strategies have been developed to ensure that the monitored target-probe binding event

Table 2
Major nanomaterials used for OTA detection (Majdinasab et al., 2015; Lawal 2018; Qiu et al., 2019, Tian et al., 2018b; Ge et al., 2017, Wang et al., 2017d, Shu and Tang 2017; Aldewachi et al., 2018).

Types		Properties	Disadvantages	Functions
CNMs	CNTs	One-dimensional atomic sheet structure Large surface area (1315 m^2/g) Chemical and thermal stability High electrical conductivity Mechanical strength	Possible toxicity Low solubility in common solvents Easy to reunion in some matrixes Same with CNTs	Fluorescence quenchers Electrode modifiers
	Gr/GO/rGO	Two-dimensional atomic sheet structure High electrical conductivity (60-fold greater than CNTs) Large surface area (2630 m^2/g), Energy acceptance ability Mechanical strength High thermal conductivity Cheaper production than CNTs Facile functionalization and biocompatibility		Fluorescence quenchers Electrode modifiers Energy acceptors
	GQDs	Zero-dimensional atomic Small size ~100nm Low cytotoxicity High water solubility Non-zero band gap Excellent biocompatibility Excellent photostability Robust chemical inertness Low cost preparation	Narrow spectral coverage Low product and quantum yield Confusing photostability mechanism	Fluorescent probe
MBs/MNP		Super paramagnetic Controllable size Easy functionalization Physicochemical stability	Modification required	Signal amplification Sample pre-concentrators Electrode modifiers Substrates for the immobilization of antibody or antigen
MNs	MONPs	One-dimensional morphology High electronic conductivity Physicochemical stability High specific surface area	Possible toxicity	Signal enhancers in the electrochemical biosensors Electrode modifiers Fluorophore Fluorescence emission Fluorescence quenchers
	AuNPs/AgNPs/ Cu NPs	High extinction coefficients Good stability and conductivity Size related electronic, magnetic and optical properties Excellent biocompatibility High surface area-to-volume ratio Easy functionalization	Low stability in high ionic strength samples Lack of integration capability into simple platforms	Signal enhancers in EC biosensors Electrode modifiers Fluorescence probes Fluorescence quenchers SERS signal amplifiers Substrate and amplification Labels in the SPR Energy acceptors
QDs		High quantum yield High molar extinction coefficients Broad absorption spectra Narrow and symmetric emission bands (30–50 nm) High resistance to photo-bleaching and chemical degradation	Intrinsic toxicity Unproductive due to antibody binding Difficult to control of dispersity of QDS size	Electrochemical labels Fluorescence labels
UCNPs		High resistance to photobleaching and photoblinking Long lifetime, and sharp emission bands. Low toxicity High color purity Multicolor tunable properties High chemical stability Robust photo-stability Low background fluorescence	Low background signals Low upconversion luminescence efficiency Possible toxicity	Fluorescent labels Signal report in NIR (near infrared) and LRET (luminescence resonance energy transfer) Energy donor
MOFs		High specific surface areas Tunable pore sizes Exposed active sites Superior catalytic activities Simple synthesis methods	Poor chemical stability	Ideal immobilization matrix Fluorescence quenchers Signal amplification in the EC biosensor

generate a measurable sensor response. Direct detection assay can only be suitable for analyte detection with molecular weight greater than 5 kDa. For low-molecular-weight analytes such as OTA (403,8 Da), the sufficient signal is not always provided due to the insignificant change of the refractive index. Therefore, two typical major approaches: AuNPs based surface modification and phase sensitive based signal enhancement (Mahmoudpour et al., 2019), are considered for SPR signal enhancement. For the first strategy, Karczmarczyk et al. (2016) developed a fast and sensitive SPR immunoassay based on competitive AuNPs for OTA detection in red wine. The reported biosensor allowed for OTA detection at a LOD of 0.068 ng/mL by applying AuNPs as a signal enhancer while that of 0.75 ng/mL without signal enhancer. Lee et al. (2018) demonstrated the first aptamer-modified gold nanorods (AuNRs) based LSPR optical-fiber sensor. As shown in Fig. 6 B, AuNRs are immobilized on a thiol-functionalized unclad fiber core followed by the modification of specific aptamers of OTA with a thiol group at their 5′-end. When the aptamer-AuNRs modified optical fiber was dipped into OTA solution, the configuration of aptamer transformed into a GQx

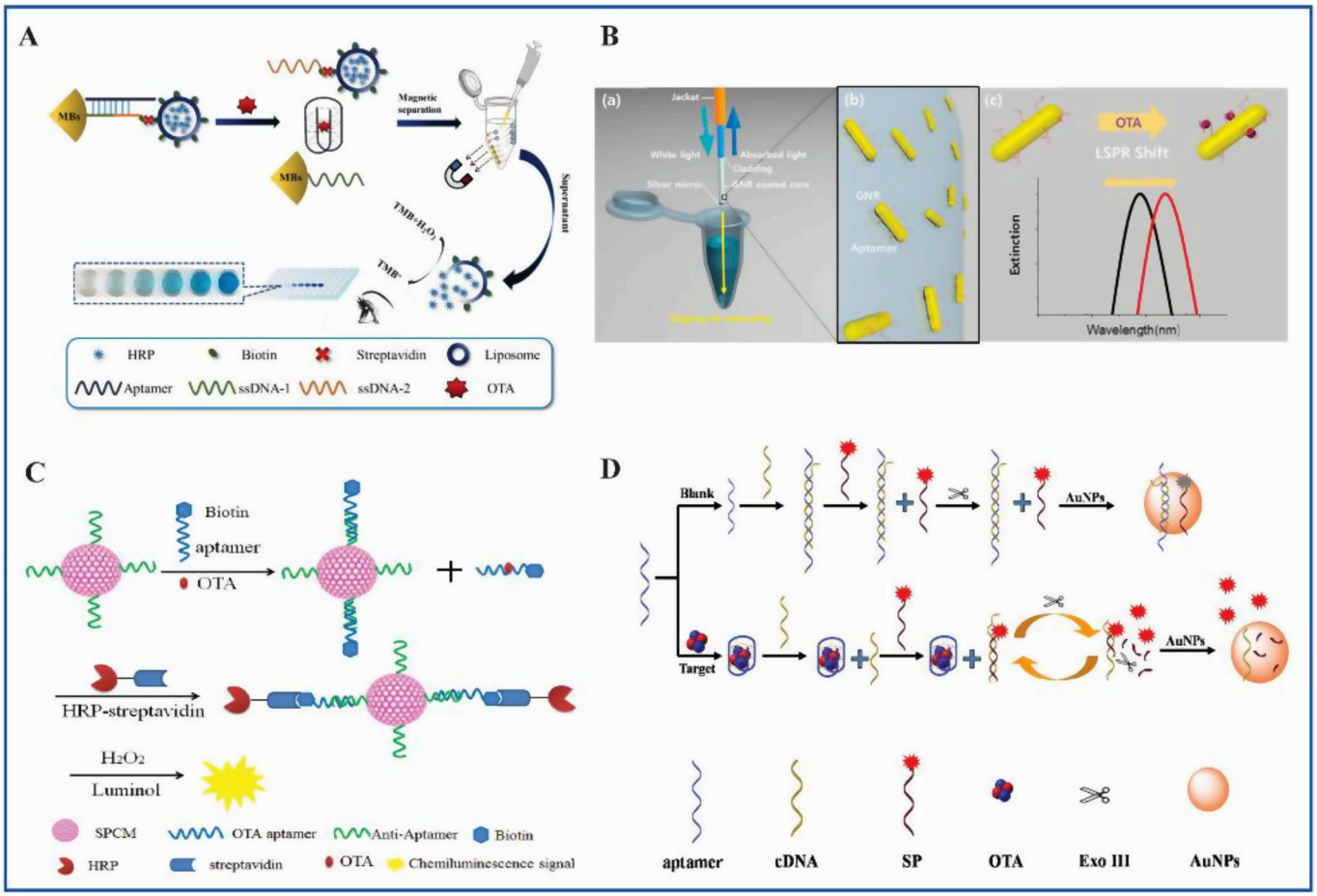

Fig. 6. The principle of the (A) colorimetric aptasensor for OTA detection based on HRP-encapsulated liposomes; (B) the optical fiber-based LSPR aptasensors; (C) chemiluminescence aptasensor based on competitive assay; (D) Exo III aided amplification fluorescence assays. The figures are reproduced from Ref (Lin et al., 2018 (A), Lee et al., 2018 (B), Shen et al., 2018 (C), Zhao et al., 2018 (D)).

structure due to the OTA/aptamer binding inducing a red shift of AuNRs LSPR peak. The LSPR peak shift displayed a linear response (R^2 = 0.9887) to OTA in the concentration range of 10 pM to 100 nM with a LOD of 12.0 pM. This method could resolve the instability problem of colloidal NPs at certain levels of pH and salts without any interference from other mycotoxins. Moreover, this approach provides over 100-fold greater sensitivity than the regulation limit (0.5 ppb), allowing for real time sensing (~30 min) with good recovery of 85.5%-116.9%. The second phase-sensitive based SPR signal enhancement strategy (SPR-polarization platform) adopting aptamer as bio-receptor was reported by Bianco et al. (2017). Two different immobilization strategies for modifying the aptamer onto SPR sensor surface which were direct (SAMs) and in presence of an aliphatic spacer (mixed SAMs) were compared in this SPR-polarization platform for OTA detection. Results showed that the sensitivity of SAMs layer was considerably higher than the mixed ones, allowing a LOD of 0.005 ng/mL in buffer and screening in food matrices at levels in the range of the EU limits. Nevertheless, a purification/concentration of the extracts or pretreatment of sample with binding agent such as PVP was required before their detection to increase the sensitivity or reduce non-specific adsorption in the above studies.

3.1.3. Chemiluminescence-based biosensors

Chemiluminescence (CL) is a very useful tool for quantification of biological materials, because of its wide linear range, high sensitivity, simple reagent preparation, stability and short assay time (Wang et al. 2010, 2016d). CdTe QDs, exonuclease-catalyzed target recycling amplification (Yang et al., 2014a), loop-mediated isothermal amplification (LAMP) (Yuan et al., 2014), chemiluminescence resonance energy transfer (CRET) (Jo et al., 2016), and silica photonic crystal microsphere (SPCM) (Shen et al., 2018) were used to enhance the CL signals for OTA screening. For instance, CdTe QDs were used to enhance the ECL emission of the $(bpy)_3^{2+}$tripropyl amine (TPrA) system combining the MIP as the selective biorecognition element with a low LOD of 3.0 fg/mL. This ECL sensor has also been applied to detect OTA in corn and human serum samples with satisfied results after simple treatment in a good recovery range of 85.1% - 107.9% (Wang et al., 2016d). Shen et al. (2018) designed a competitive aptamer-based CL biosensor by using SPCM strategy to detect OTA in cereals (Fig. 6 C). The competition of OTA and aptamers binding reaction was performed between anti-aptamer immobilized on surface of SPCM and OTA in the sample. The presence of OTA in the sample would bind to the necessary aptamer, limiting it from hybridization with anti-aptamer and decreasing the CL signal of microspheres which was developed by HRP streptavidin, luminol and H_2O_2 system. The LOD of 1.0 pg/mL and high selectivity towards OTA against other mycotoxin was obtained in this system. The recovery range in the cereals sample were 81% to 105%, indicating reliable OTA detection in real samples.

4.1.4. Fluorescence-based biosensors

Fluorescence is considered as the most applied and powerful optical method in medical diagnostics, drug discovery, environmental monitoring, and food safety because of its great versatility, non-destructive tracking, and multiplexed ability (Jeong et al., 2018). Fluorescence-based biosensors employing aptamer and antibodies associated with different nanomaterials such as MBs, AuNPs, CuNPs have been

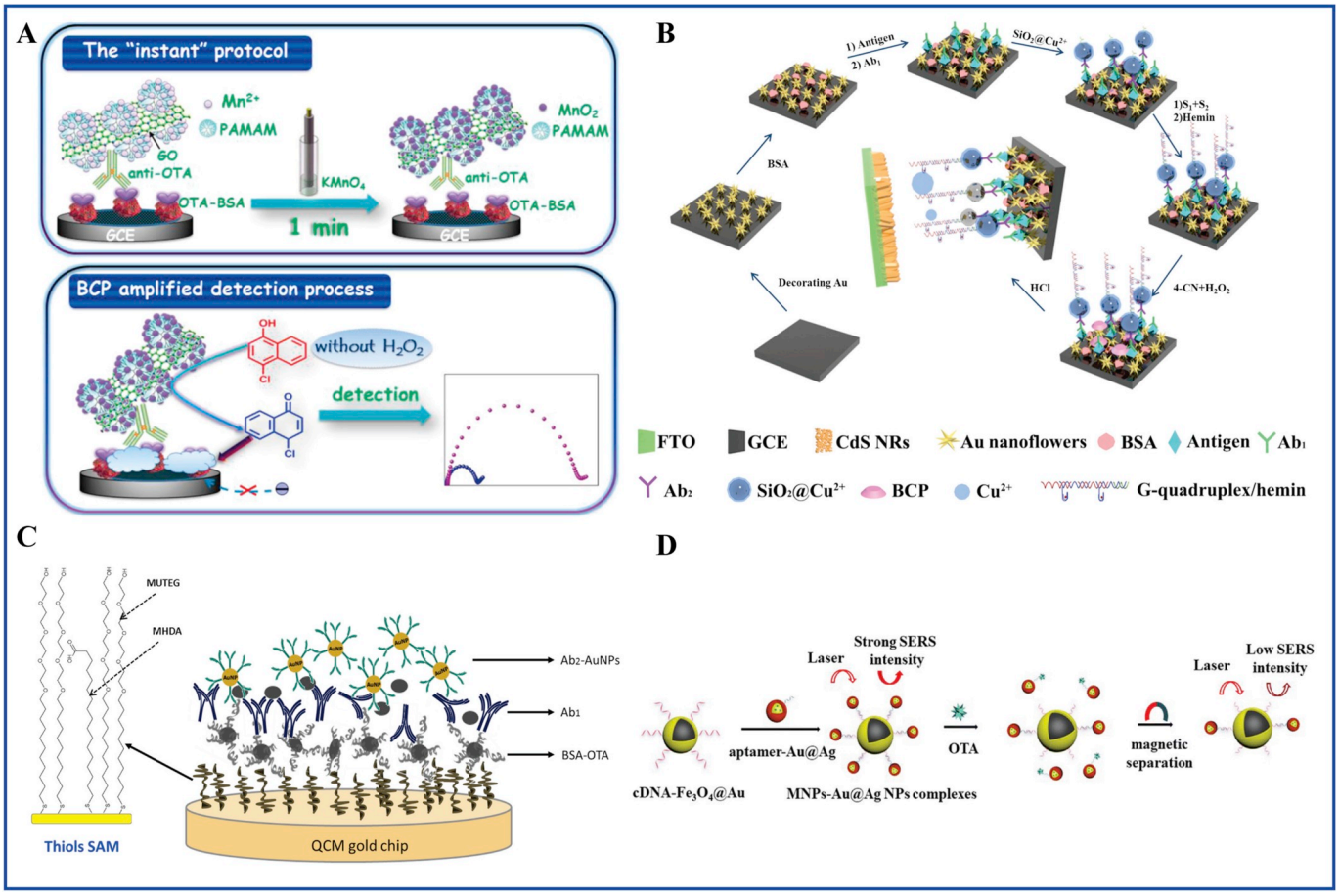

Fig. 7. Schematic representations of (A) the instant protocol and the BCP amplified impedimetric detection of OTA; (B) illustration of PEC immunosensor of OTA; (C) competitive immunoassay utilizing QCM based detection of OTA; (D) principle of the SERS based aptasensor for OTA detection. The figures are reproduced from Ref (Tang et al., 2016 (A), Qileng et al., 2018 (B), Karczmarczyk et al., 2017b (C), Song et al., 2018(D)).

presented for the determination of OTA. MBs-based biosensor for OTA detection is simple, rapid and efficient, and without the need of multiple separation steps and excessive washing (Mahdi et al., 2016). Magnetic silica NPs labeled with rhodamine 123 (Rho123) was used as the signal intensifier in a CdTe QDs based immunoassay for OTA detection. The immune reaction between anti-OTA antibody and OTA brought the fluorophore (acting as the acceptor) in a proximity to the QDs (acting as the donor) causing FRET to occur upon photoexcitation of the QDs. This method has a LOD of 0.8 pg/mL of OTA. HCR amplification strategy was used to help achieve an ultrasensitive detection of OTA in corn samples (Wang et al., 2016a). In this design, positively charged perylene derivative ((N,N-bis (propylenetrimethylammonium)-3,4,9,10-perylenediimide), PAPDI) served as the fluorescent probe, while dendritic DNA concatamers synthesized by HCR strategy and modified on MNPs through aptamer as medium was used to induce the aggregation of PDI probe, which further amplified the detection signal. The LOD of the proposed aptasensor was 0.10 pM. Another case using MBs in fluorescence aptasensor was reported by Qian et al. (2018), allowing simultaneous determination of OTA and AFB1 in a single analytical run a LOD of 0.67 and 1.70 pg/mL for OTA and AFB1, respectively.

The ability of AuNPs to exhibit FRET drove Lv et al. (2018) to develop a simple and selective biosensor by using AuNPs as quenchers of FAM-modified aptamer. The presence of OTA in the system bound to the fluorescent dye labeled aptamer to form a folded structure which resisted the adsorption of FAM-modified aptamer on AuNPs which induced a fluorescent signal. The LOD of this sensing platform was 5 nM. Exonuclease III (Exo III) was used for signal amplification in AuNPs quenching fluorescence detection platform for OTA (Zhao et al., 2018). The aptamer first recognized and bound to OTA, thus leads to the formation of duplex DNA between the cDNA strand and the signal probe. Exo III then digested the duplex DNA from the 3′ blunt terminus of the signal probe to liberate the fluorophore and release cDNA. The released cDNA then hybridized with other signal probes to initiate a new cleavage reaction. Through this cyclic hybridization-hydrolysis process, an OTA molecule can trigger the cleavage of a large quantity of signal probes. Upon the addition of AuNPs, the fluorophore cannot be adsorbed and quenched, resulting the amplified fluorescence signal (Fig. 6 D). The designed aptasensor was highly selective for OTA with a LOD of 4.82 nM. Lower LOD of 2.0 nM with outstanding specificity towards OTA in red wine was obtained using an enzymatically generated polythymine-coated CuNPs based fluorescent aptasenor (He et al., 2019). The OTA-binding aptamer was first immobilized on MBs and partially released and exposed a region with cDNA at the presence of OTA. After magnetic separation, the cDNA was employed as a primer to trigger the terminal deoxynucleotidyl transferase-mediated polymerization. The process generated polythymine as a template for synthesis of the CuNPs and caused the fluorescence signal. However, the intensity is smaller in the diluted red wine without any pretreatment than in the buffer, which may result from the interference of the complex molecules in red wine for CuNP formation.

4.2. Electrochemical biosensors

For EC biosensors, the EC parameters (potential, impedance, or current) of the sensing electrode change when analytes present in the

sample (Wang et al., 2016c). Electrochemistry has been widely used in various fields, due to their high selectivity and sensitivity, high signal-to noise ratio, simplicity, miniaturization, low cost, robust to liquid samples and more feasible for on-site application. All kinds of nanomaterials and bio-receptors introduced previously coupled with amplification strategies such as LAMP (Xie et al., 2014), two-level cascaded signal amplification strategy with methylene blue (Yang et al., 2014b), and exonuclease-catalyzed target recycling (Tan et al., 2015; Shi et al., 2018), have been introduced into the design of EC biosensors to improve the analytical performance (Velusamy et al., 2010). Tang et al. (2016) used an instant catalyst as enhancer to develop a new impedimetric biosensor for determination of OTA in red wine. The signal tags (anti-OTA-GO-PAMAM) were prepared via co-immobilization of anti-OTA antibody and amine-terminated dendrimer (PAMAM) on the GO nanosheets through the covalent interaction to combine manganese ion (Mn^{2+}). As shown in Fig. 7 A, a competitive-type immuno-reaction was implemented between the analyte OTA and the immobilized OTA-BSA on the electrode with the anti-OTA antibody on the tags. The anti-OTA-GO-PAMAM-Mn^{2+} were captured onto the electrode surface, inducing the in-situ formation of MnO_2 via classical redox reaction between Mn^{2+} and $KMnO_4$ on the immuno-sensing platform. Also, the generated MnO_2 NPs acting as efficient catalyst could catalyze the 4-chloro-1-naphthol (4-CN) oxidation without H_2O_2. The instant catalyst based impedimetric immuno-sensor displayed a LOD of 0.055pg/mL. Voltammetry including CV, DPV, and square wave voltammetry (SWV) are attractive techniques due to their simplicity (Mishra et al., 2016). A broad-specific photo EC (PEC) immunosensor was developed for the simultaneous multiplexed detection of OTA, OTB, OTC by using the direct growth of CdS nanorods on fluorine-doped Tin oxide (FTO) as the photo electrode and Au nanoflowers-modified glass carbon electrode (GCE) as the bioelectrode (Qileng et al., 2018). As shown in Fig. 7 B, the bioelectrode was used to capture antigens by using SiO_2@Cu^{2+} nanocomposites to conjugate the secondary antibody (Ab_2) and a DNA strand as the initiator. Due to the similar enzymatic property HRP, G-quadruplex/hemin produced by HCR and hemin can accelerate the oxidation of 4-CN with H_2O_2 to yield the biocatalytic precipitation (BCP) on the bioelectrode. The bioelectrode was further treated with moderate acid, and Cu^{2+} was then released, which decreased the photocurrent of the photoelectrode by forming CuS. Due to the surface effect of Au nanoflowers, DNA amplification and high photo-electrocatalytic activity, the proposed broad-specificity PEC immunosensor can detect OTA, OTB and OTC with a LOD of 0.02, 0.04 and 0.03 pg/mL, respectively. However, much lower LOD of 0.3 fg/mL was obtained when NH_2-Co-MOF assisted substrate-free electrocatalysis of Thi with Exo I based target recycling amplification was introduced into an EC aptasensor (Wang et al., 2017e). A great deal of OTA aptamer cDNA sequences was produced with the proceeding of the Exo I-assisted OTA recycling. After that the DNA Y-junction structure was introduced onto the aptasensing interface by the hybridization of three complementary DNA sequences, and many redox molecules (Thi) could then be efficiently intercalated into DNA grooves via electrostatic adsorption and caused ultrasensitive signal change.

Discovery was also made by developing an EC aptasensor without signal amplification strategy for OTA detection with an extraordinary tunable dynamic sensing range (Cheng et al., 2017). The presented EC aptasensor was constructed based on the target induced aptamer-folding detection mechanism. The recognition between OTA and its aptamers produced conformational change of the aptamer probe along with signal changes for measurement. The dynamic sensing range of the aptasensor was successfully tuned by the introduction of free assistant aptamer probes in the sensing system. This EC aptasensor showed an extraordinary dynamic sensing range of 11-order magnitude of OTA concentration from 10^{-8} to 10^{2} pg/mg. Results showed that the OTA only or OTA in the complicated mixture could induce distinguishable current signal responses while other interferent showed negligible effect, which indicated its outstanding specificity. An amperometric sensor based graphene-MWCNTs-chitosan-ionic liquid (Gr-MWCNTs-Ch-IL)/collagen-IL (CG-IL)/NiONPs/GCE with good affinity and stability was able to achieve an ultra-sensitive OTA with a LOD of 0.5×10^{-11} nM and a sensitivity of 36.4 μA nM^{-1} (Jalalvand, 2018).

4.3. Mass-sensitivity based biosensors

A quartz crystal microbalance (QCM) biosensor is based on piezoelectric principle by the product of vibration at a definite resonance frequency (Masdor et al., 2016), and the result is measured by an electric signal applied by two gold plates (Mutlu, 2010). The detection technique doesn't require any labeling step for the signal transduction and displays detection sensitivity from 1- to 100-fold linear frequency (ΔF) vs. mass range with LOD of as low as ng/mL levels (Marx, 2003). QCM is widely used in detection of various analytes at low concentrations, such as bacteria (Yu et al., 2018b), mycotoxins (Ertekin et al., 2016), and viruses (Wang et al., 2017b), due to their simplicity, low cost, and sensitivity (Ratautaite et al., 2015). Another advantage of QCM over other endpoint measuring tools is the ability to realize real-time measurements, which makes it perfect to be used in automated continuous monitoring systems (Cimpoca et al., 2009). In an amazing and unique fashion, an immuno-sensor based on a gold-coated QCM with dissipation monitoring (QCM-D) was developed for rapid and sensitive detection of OTA in red wine (Karczmarczyk et al., 2017b). The indirect competitive assay employed made it possible to simultaneously measure frequency (Δf) and dissipation (ΔD) changes. The result provided detailed information about the mechanical and viscoelastic properties of the biofilm. A LOD of 0.16 ng/mL was achieved. Matrix effect associated non-specific interactions with the sensor surface was minimized by a simple pre-treatment of the wine with addition of binding gent PVP (Karczmarczyk et al., 2017b) (Fig. 7C). Although the researchers put efforts in construction of highly sensitive and reliable QCM-biosensors, these sensors sensitivity still do not meet the requirements, especially regarding detection of small molecules such as mycotoxins.

4.4. Surface-enhanced Raman scattering based biosensors

Surface-enhanced Raman scattering (SERS) technique, adopting noble metal NPs such as AuNPs (Li et al., 2018), AgNPs (Ganbold et al., 2014) and Au-Ag nanocomposites (Zhao et al., 2015b) as active substrates, with ultrasensitive and multiplexed detection capability, has also been applied on aptamer and antibody-based biosensors for OTA detection. The Raman effect is the basis of SERS strategy, which is an inelastic scattering of episode photons by a molecule upon brightness with electromagnetic radiation. Li et al. (2018) created AuNPs based SERS immunosensor for three mycotoxins detection (aflatoxin B1, AFB1; zearalenone, ZEA; ochratoxin A, OTA) in foodstuff. In this study, AuNPs were labeled with 5,5-dithiobis (succinimidyl-2-nitrobenzoate) (DSNB) as Raman reporter and covalently linked with anti-mycotoxin Abs as SERS nanoprobes, while AFB1-BSA, ZEA-BSA, and OTA-BSA conjugates were covalently linked onto microarray gold surface as corresponding capture substrates. This design allows three independent multiplexed immunoreactions on a single gold chip. The LOD were 0.061-0.066 μg/mg for AFB1, 0.53-0.57 μg/mg for ZEA, and 0.26-0.29 μg/mg for OTA in food stuff. MNPs was utilized to collect Raman signals from samples in an effective and recyclable way during the detection procedure. Song et al. (2018) developed a fascinating aptasensor for OTA detection by combining DTNB embedded Au@Ag NPs with MNPs (MGNPs). Au-DNTB@Ag NPs modified with OTA aptamer (aptamer-GSNPs) were used as molecular recognition and Raman signal probes for the first time. As shown in Fig. 7. D, MGNPs modified with cDNA (cDNA-MGNPs) were considered as both capture probes and SERS signal reinforced substrates. When the aptamer-GSNPs were mixed with cDNA-MGNPs and Au-DTNB@Ag-Fe_3O_4@Au, they produced complexes through oligonucleotide hybridization resulting in

Table 3
Summary for different read-out OTA biosensors.

Different read-out biosensors		Bioreceptors	Nanomaterials	LOD (ng/mL)	Linear range (ng/mL)	Analysis time (min)	Sample pretreatment	Recovery (%)	Specificity	Samples	References
Optical	Colorimetric	Aptamers and DNAzyme	/	0.004	0.004–0.129		Double LLE and solvents extraction			Yellow rice wine and wheat flour	Wang et al. (2015a)
			Au NRs	4.03	4.03–80.76	~90	/	/	High selectivity	Beer	Yu et al. (2018c)
		Aptamer	Au NPs	0.02	0.08–100.95	~3[a]	Extraction	/	High specificity	Red wine	Xiao et al. (2015)
			Au@Fe_3O_4 NPs	0.03	0.5–100	~90	/	/	/	Peanut, corn	Wang et al. (2016b)
			Au NPs	20.0	32 ~ 1024	~25	Evaporative, and solvent extraction	100.80–112.50	Excellent selectivity	Fortified white grape wine	Yin et al. (2017)
			Au NRs	0.22	0.5–20	~60[a]	Solvent extraction	92.0–118.2	Good selectivity	Red wine	Xu et al. (2016)
			Au NPs	0.009	0.05–50	~20	Without	/	High selectivity	Chinese liquor (Maotai)	Luan et al. (2015)
			MBs	0.023	0.05–2.0	~60[a]	Solvent extraction	98.5–106.1	High selectivity	Corn	Lin et al. (2018)
		Antibody	Au-N-TiO_2	28×10^{-6}	0.0001–1	/	/	97.8–100.6	Acceptable	/	Ren et al. (2018)
	Lateral flow assay	Aptamer	Au NPs	1.0	/	~15	Solvent extraction	/	Excellent selectivity	Astragalus membranaceus	Zhou et al. (2016)
			UCNPs	1.86	5 ~ 100	~15	Filtration and solvents extraction	88.4–95.9	High selectivity	Wheat, beer	Wu et al. (2018b)
			/	0.40	1 ~ 1000	~20	Solvents extraction and centrifugation	/	Good specificity	Corn	Zhang et al. (2018)
		Antibody	Au NPs	0.91	0 ~ 25	/	/	/	/	/	Li et al. (2016)
			Ag NP, Ru NPs	60	80 ~ 5000	~20	Dilution	88.0–110.0	Good specificity	Grape juice, wine	Jiang et al. (2017)
	CL	Aptamer	SiO_2 NPs	3.0×10^{-4}	10^{-3} ~ 50	/	Solvents extraction and filtration	97.0–105.0	Acceptable	Wheat	Hun et al. (2013)
			/	10^{-3}	10^{-3} ~ 1	~220	Solvents extraction and filtration	81 ~ 105	Good specificity	Cereal	Shen et al. (2018)
	CRET	Aptamer-DNAzyme	/	0.22	0.1–100	~63	Solvents extraction and filtration	71.5–93.3	Acceptable	Coffee	Jo et al. (2016)
		DNAzyme–aptamer	/	0.27	/	~15	Without	/	Acceptable	Espresso coffee	Mun et al. (2014)
	ECL	aptamer	/	0.02×10^{-3}	0.05×10^{-3} ~ 0.5	/	Solvents extraction	91.4–98.5	Good selectivity	Corn	Yang et al. (2015b)
		MIP	Ru Si NPs	3×10^{-6}	1×10^{-5} ~ 11.13	~5[a]	Corn: Solvents extraction and centrifugation Serum: dilution	85.1–107.9	Acceptable	Corn, human serum	Wang et al. (2016d)
			RuSi NPs, CdTe QDs	0.027×10^{-3}	0.1×10^{-3}-14.76	~130	Solvents extraction, centrifugation and dilution	95.3–99.3	Acceptable	Corn	(Wang et al., 2016e)
	SPR	Aptamer	/	0.005	0.094–10	/	Liquid–liquid extraction	86.92–116.54	Good selectivity	Wine, peanut oil	Zhu et al. (2015)
		Antibody	AuNPs	0.75	/	~55	3% PVP	/	/	Red wine	Karczmarczyk et al. (2016)

(*continued on next page*)

Table 3 (*continued*)

Different read-out biosensors	Bioreceptors	Nanomaterials	LOD (ng/mL)	Linear range (ng/mL)	Analysis time (min)	Sample pretreatment	Recovery (%)	Specificity	Samples	References
		CS-Au/CMC-Au	5.7 CS 3.8 CMC	0 ~ 50	/	Solvents extraction	/	Good	Coffee	Rehmat et al. (2019)
	SPR, QCM	Aptamer	/	0.005	down to 0.2	~210	/	/	/	/	Bianco et al. (2017)
	LSPR	Aptamer	Au NRs	4.8×10^{-3}	0.004–40.38	~30	Dilution	85.5–116.9	High selectivity	Grape juice	Lee et al. (2018)
				0.4×10^{-3}	$0.4 \times 10^{-3} \sim 0.04$	/	/	/	/	/	Yim et al. (2015)
				0.40	$0.04–4 \times 10^{3}$	~50	Solvents extraction	108.3–109.4	High selectivity	Ground corn	Park et al. (2014)
	Fluorescence	Aptamer	Au NPs	1.946	/	~145	Without	96 ~ 112	Outstanding specificity	Red wine	Zhao et al. (2018)
				2	4.081–403.81	~190	Solvents extraction and filtration	89.0–117.8	High specificity	Ginger powder	Lv et al. (2018)
			Nitrogen doped carbon dots (CD), Ag NPs	3.513	4.038–20.19	~33	Solvents extraction and filtration,	98.7–113.1	Good specificity	Flour, beer	Wang et al. (2018a)
			CeO_2NPs, GQDs	2.5×10^{-3}	0.01–20	/	Solvents extraction	90 ~ 110	Outstanding specificity	Peanuts	Tian et al. (2018)
			Fe_3O_4/g-C_3N_4/HKUST-1	2.57	5.0–160.0	~60	Solvents extraction, filtration, and magnetic separation	/	Good selectivity	Corn	Hu et al. (2017)
			QDs-MoS_2 nanosheets	1.0	1.0–1000	~40[a]	Solvents extraction	92 ~ 123	High binding affinity and specificity	Red wine	Lu et al. (2017)
			SYBR Gold	6.66	/	~60	Without	93.6–107.9	High selectivity	Red wine, beer	Lv et al. (2017b)
			TiO_2 NPs	0.605	0.605–403.8	~101	Degassed, filtration, dilution	94.30–99.20	High selectivity	Beer	Sharma et al. (2015)
			SWCNHs	6.945	8.076–201.9	~30	Without	93 ~ 104.9	High selectivity	Red wine	Lv et al. (2016)
			nano-graphite	8.076	8.076–161.5	~130	Without	101.3–104.0	Good selectivity	Red wine	Wei et al. (2015)
			SNPs, AuNPs	0.039	0.06–2.422	/	/	/	/	Grape juice, serum	Taghdisi et al. (2016)
			Fe_3O_4@Au MBs, CdTe QDs, SiO_2 nanocarrier	5.4×10^{-3}	0.015–100	~60	Magnetic separation	96.0–99.7	High selectivity	Peanut	Wang et al. (2015b)
			Ag NCs-MBs	0.002	1.0–100	~17	Extraction filtration and magnetic separation	93 ~ 108	Ultra-high selectivity	Wheat	Chen et al. (2014)
			MNs, QDs	0.13×10^{-3}	$10^{-3} \sim 10$	~80	Magnetic separation	/	Excellent specificity	Red wine	Yao et al. (2015)
			MBs	0.002	0.04–60.57	~110	Degassed, filtration, magnetic separation	96 ~ 97.5	Good specificity	Beer	Hayat et al. (2015)
			Cu NPs-MBs	0.81	1 ~ 101	~190	Without	/	Outstanding specificity	Red wine	He et al. (2019)
			Ag NCs	0.2×10^{-3}	0.001–0.05	~35		88.5 ± 6.90-113.5 ± 5.30	Ultra-high selectivity	Wheat, rice, corn	Zhang et al. (2016a)

(*continued on next page*)

Table 3 (*continued*)

Different read-out biosensors		Bioreceptors	Nanomaterials	LOD (ng/mL)	Linear range (ng/mL)	Analysis time (min)	Sample pretreatment	Recovery (%)	Specificity	Samples	References
							Solvents extraction centrifugation, filtration, and magnetic separation				
			MNPs	0.04×10^{-3}	$0.4\times10^{-3}\sim0.008$	~60[a]	Solvents extraction, and magnetic separation	96.0–101.5	Sufficient selectivity	Corn	Wang et al. (2016a))
			SiO_2 NPs	0.20-0.02	/	~60	Solvents extraction centrifugation	93.05–96.28	Good selectivity	Wheat	Ribes et al. (2017)
			GQD	0.013	0 ~ 1	~120	Filtration	94.4–102.7	High selectivity	Red Wine	Wang et al. (2017c)
			Au NPs	9.166	10.09–121.14	~58	Corn: Solvents extraction centrifugation; Beer, coffee: dilution	90.2–113.2	Good selectivity	Corn, beer, coffee	Lv et al. (2017c)
			Fe_3O_4@AuM-B, CdTeQDs, silica NPs	0.67×10^{-3}	0.002–5	/	/	95 ~ 108	Acceptable	Corn	Qian et al. (2018)
		Aptamer/ DNase I	SWCNH	3.96	4.04–80.76	~120	Without	93 ~ 106	High specificity	Red wine	Lv et al. (2017a)
		Antibody	CdTe QDs	7.06×10^{-3} and 4.15×10^{-3}	7.06×10^{-3} ~18.34 and 4.15×10^{-3} ~4.88	/	Magnetic purification	94 ± 6.3–106 ± 0.7	High specificity	Red wine	Yao et al. (2017)
	FRET	Aptamer	Au NP, CdTe QDs	1.67×10^{-3}	0.01–5	~60 [a]	Simple filtration	94.0–97.3	High specificity	Red wine	Qian et al. (2015)
			CdSe/CdS QDs	0.5	1 ~ 30	5	Dilution	/	High selectivity	Beer	Chu et al. (2016)
			Au NPs	2.019	4.038–403.8	~190	Solvents extraction, centrifugation, filtration	89.0–117.8	High specificity	Ginger	Lv et al. (2018)
		Antibody	Magnetic silica NPs, CdTe QDs	0.8×10^{-3}	0.008–0.048	~3	Without	/	/	Human serum	Mahdi et al. (2016)
EC	Impedimetric	Aptamer	Au NPs–carboxylic porous carbon (cPC)	10^{-8}	$10^{-8}\sim0.1$	~9 [a]	/	95 ~ 108	Good specificity	Soybean	Wei and Zhang (2017)
			IrO_2 NPs	0.0056	0.004–40.381	~90 [a]	Without	125	High specificity	White wine	Rivas et al. (2015)
			Au NPs-rGO	0.03	0.1–200	90 [a]	simple pretreatment, filtration	91.0–97.1	High selectivity	Red wine	Qian et al. (2014)
			Au NPs-rGO	0.3×10^{-3}	0.001–50	~180	Filtration, dilution	90 ~ 97	/	Red wine	Jiang et al. (2014)
		Antibody	GO-AMAMMn^{2+}	0.055×10^{-3}	$0.1\times10^{-3}\sim0.03$	~51	Without	96.8–106.5	High selectivity	Red wine	Tang et al. (2016)
			AuNPs	0.25	0.3–20	~50	I'Screen ochra ELIZA kit	94.56–102.91	/	Red wine	Malvano et al. (2016a)
	Amperometric	/	NiO NPs Gr-MWCNTs	0.002	0.004–4.038	~20	Filtration and centrifugation	96 ~ 104.6	Good selectivity	Juice	Jalalvand (2018)
	Voltammetric	Aptamer	GONPs nanoplatelets	0.125×10^{-3}		~80	/	/	High selectivity	/	Loo et al. (2015)

(*continued on next page*)

Table 3 (*continued*)

Different read-out biosensors	Bioreceptors	Nanomaterials	LOD (ng/mL)	Linear range (ng/mL)	Analysis time (min)	Sample pretreatment	Recovery (%)	Specificity	Samples	References
				0.125 $\times 10^{-3}$ ~ 0.125						
		$MoSe_2$/AuNPs, MB	0.032×10^{-3}	0.04×10^{-3} ~ 0.40	~46	Without	96.2–104.3	Good selectivity	Wine	(Huang et al., 2016)
		SiO2@Au, CdTe QDs, GAu/CdTe	0.07×10^{-3}	0.2×10^{-3} ~ 4	~90	/	/	High selectivity	/	Hao et al. (2016)
		/	0.07	0.15-5	~80	(MIP) columns	82.1–85	High selectivity	Cocoa	Mishra et al. (2016)
		f-graphene-CS	1×10^{-7}	1×10^{-6} ~ 1000	~8	Without	90 ~ 101	High specificity	Grape juice	Kaur et al. (2019)
		Ag NPs	0.02	0.028–4.038	~180	/	/	Highly specificity	/	Karimi et al. (2017)
		cPC and AuNPs, MB	5.0×10^{-6}	5.0×10^{-6} ~ 5.0×10^{-4}	~15[a]	/	90 ~ 114	Acceptable	Corn	Wei and Feng (2017)
		Co/Fe-MOFs	0.3×10^{-6}	10^{-6} ~ 1.0	/	/	/	Satisfactory selectivity	/	Wang et al. (2017e)
		Au NPs-MB	0.3×10^{-3}	0.001–1.009	~40	Filtration, dilution	90 ~ 95	High selectivity	Red wine	Yang et al. (2014b)
	Aptamer/DNase I	GO nanosheets	5.6×10^{-3}	0.01–50	~90	Solvents extraction, filtration	/	Acceptable	Wheat	Sun et al. (2017)
	Antibody	zirconium dioxide–reduced graphene oxide (ZrO_2-RGO)	0.079	1 ~ 20	~25[a]	Ultra-sonication	95.6–98.2	Acceptable	Coffee	Gupta et al. (2017)
	Minotope peptide-antibody	Au NPs	2.04×10^{-6}	7.17×10^{-6} ~ 0.548×10^{-3}	~120 [a]	Corn samples: Solvents extraction, centrifugation Beer samples: extraction and filtration	89.6–107.4 99.3 ~ 104.3	Highly specificity	Beer, corn	Hou et al. (2018)
	MIP	MWCNTs	5.65	20.19–403.81	~15	Without	84–110	/	Beer, wine	Pacheco et al. (2015)
		AgNPs/POM (polyoxometalate)/rGO	0.0064	0.02–0.6	/	Filtration and dilution	~100.00	Good selectivity	Grape juice, win	Yola et al. (2016)
	/	Au NPs	0.08	0.20–4	~3[a]	Solvents extraction, filtration Beer: boiled	82.0–108.0	/	Breakfast cereal, cereal-based baby foods, beer	Afzali et al. (2016)
Photoelectrochemical (PEC)	Antibody	CdSe NPs, TiO_2 NPs	0.002	0.01–50	/	/	98.6–107.9	Good selectivity	Milk	Yang et al. (2015a)
		TiO_2/S-$BiVO_4$@Ag_2S	1.7×10^{-3}	0.005–750	/	/	99.25–101.4	Excellent selectivity and specificity	Red wine	Feng et al. (2018)
		CdS nanorods on FTO, SiO_2@Cu^{2+}	0.02×10^{-3}	0.0002–0.1	~340	Without	95 ~ 112	Acceptable	Water	Qileng et al. (2018)

(*continued on next page*)

Table 3 (*continued*)

Different read-out biosensors	Bioreceptors	Nanomaterials	LOD (ng/mL)	Linear range (ng/mL)	Analysis time (min)	Sample pretreatment	Recovery (%)	Specificity	Samples	References
		nanocomposites								
	EIS, CV, DPV	Np-Au	5×10^{-3}	0.01–5	~1230	Common filtration	98.5–105.0	Excellent selectivity	Red wine	Shi et al. (2018)
	Extraordinary tunable dynamic range, EIS, CV, DPV	/	10^{-8}	10^{-8}~10^{2}	/	Solvents extraction, and common filtration	92.1–113.8	Outstanding specificity	Red wine, maize	Cheng et al. (2017)
QCM	QCM-D	Au NPs	0.16	0.2–40	~55	3% PVP	/	Acceptable	Red wine	Karczmarczyk et al. (2017b)
SERS	Antibody	Au NPs	0.26×10^{12}~0.29×10^{12}	5×10^{-3}~5	~82	Solvents extraction, centrifugation	83.8–108.1	Acceptable	Corn, rice, wheat	Li et al. (2018)
	Aptamer	Au-DTNB@Ag-Fe_3O_4@Au	0.48×10^{-3}	1.20×10^{-3}~3.31×10^{3}	/	Without	80~110	High specificity	Wine, coffee	Song et al. (2018)
		Ag NPs	/	0.04–4	~30	Without	/	/	/	Ganbold et al. (2014)
		Ag@Au NPs	0.006	` 0.01–100	~120[a]	Solvents extraction, filtration	95.00 ± 3.08 ~ 99.48 ± 3.79	Acceptable	Maize	Zhao et al. (2015b)

[a] Represents the time without sample pretreatment time;/represents not mentioned.

high Raman signal intensity. In the presence of OTA, the crucial region of OTA aptamer selectively bound to OTA resulting in dissociation of aptamer-GSNPs probes from cDNA-MGNPs. The detected Raman signal intensity significantly decreased after magnetic separation because the relationship between OTA concentration and Raman signal intensity are inversely proportional to each other. Under the optimal conditions, the LOD was obtained as low as 0.48 pg/mL. SERS-based biosensors are more sensitive than conventional technique, however, the reproducibility still is a major obstacle for real sample detection and the availability of hand-held SERS detector with high sensitivity are factors limiting the wide application.

Applications of different read-out biosensors which are not addressed detailed above are listed in the Table 3 for a comprehensive understanding, including the important parameters for biosensors such as bioreceptors, nanomaterials, LOD, detection linear range, analysis time, sample pretreatment, recovery rate, specificity, and target samples.

5. Conclusions and future perspectives

The modern concepts of biosensors for OTA detection have been presented as a flexible and viable option to replace previous complex, expensive and time-consuming procedures. Great progress in the utilization of bio-receptors such as antibodies/nanobodies, peptides, MIPs, aptamers and DNAzymes in the field of biosensors for detection of OTA and mycotoxins has been made. However, false-positive results suffered from the lack of specificity of bio-receptors are more frequently reported in different cases: ① Sample's conditions including temperature, pH, sample viscosity, and ionic strength, influence binding activity of most types of bioreceptors; ② Cross-reactions of bioreceptors between molecules that mimic OTA in their structure or properties such as OTB, OTC, zearalenone, fumonisin B1, deoxynivlenol, warfarin, and vomitoxin or interferents such as flavonoids and phenolic compounds; ③ Non-specific interaction with a reporter molecule (e.g. biotin, dye, enzyme); ④ Non-specific adsorption from matrix effects might lead to significant overestimation of mycotoxin concentration. Significant efforts integrating nanomaterials (CNMs, MBs and MNPs, MNs, QDs, UCNPs, MOF) with bio-receptors have been devoted to offer excellent performances of OTA biosensors with high sensitivity and specificity. However, these biosensors are merely confined within laboratory investigation until now. There is still a huge challenge to make these great discoveries available to the public who urgently need an intelligent, reliable and rapid sensing tool. Hence, we propose further research perspectives in this field should focus on:

(1) To empower quick and large-scale production of nanomaterial-based biosensors with relatively low costs, excellent features and easy implement with miniatured devices.
(2) To overcome the lack of specificity of bio-recognition elements by combining various kinds of bioreceptors or nanomaterials to biosensors.
(3) To improve the sensitivity of OTA from the matrix effect of samples by integrating effective separation techniques such as magnetic separation using MNPs and MBs.

Declaration of interests

The authors declare that they have no known competing financial interests or personal relationships that could have appeared to influence the work reported in this paper.

The authors declare the following financial interests/personal relationships which may be considered as potential competing interests:

CRediT authorship contribution statement

Yasmin Alhamoud: Writing - original draft, Writing - review & editing. **Danting Yang:** Conceptualization, Writing - original draft, Writing - review & editing, Supervision, Funding acquisition, Writing - original draft, Writing - review & editing. **Guozhen Liu:** Writing - original draft, Writing - review & editing. **Linyang Liu:** Writing - review & editing. **Haibo Zhou:** Writing - original draft, Writing - review & editing. **Fatma Ahmed:** Writing - review & editing. **Jinshun Zhao:** Writing - original draft, Writing - review & editing, Supervision.

Acknowledgment

This work is funded by Natural Science Foundation of Zhejiang Province (grant number: LY17H260003), Ningbo Natural Science Foundation (grant number: 2017A610226), Science Program of Ningbo University (grant number: XYL17021) and K.C. Wong Magna Fund in Ningbo University.

References

Afzali, D., Fathirad, F., Ghaseminezhad, S., 2016. J. Food Sci. Technol. 53 (1), 909–914.
Ajeet, K., Pratima Rathee, S., Anees Ahmad, A., Sharif, A., Bansi Dhar, M., 2009. Nanotechnology 20 (5) 055105.
Aldewachi, H., Chalati, T., Woodroofe, M.N., Bricklebank, N., Sharrack, B., Gardiner, P., 2018. Nanoscale 10 (1), 18–33.
Andrade, M.A., Lanças, F.M., 2017. J. Chromatogr. A 1493, 41–48.
Ashley, J., Shahbazi, M.-A., Kant, K., Chidambara, V.A., Wolff, A., Bang, D.D., Sun, Y., 2017. Biosens. Bioelectron. 91, 606–615.
Badie Bostan, H., Danesh, N.M., Karimi, G., Ramezani, M., Mousavi Shaegh, S.A., Youssefi, K., Charbgoo, F., Abnous, K., Taghdisi, S.M., 2017. Biosens. Bioelectron. 98, 168–179.
Bazin, I., Tria, S.A., Hayat, A., Marty, J.L., 2017. Biosens. Bioelectron. 87, 285–298.
Bianco, M., Sonato, A., De Girolamo, A., Pascale, M., Romanato, F., Rinaldi, R., Arima, V., 2017. Sensor. Actuator. B Chem. 241, 314–320.
Breaker, R.R., Joyce, G.F., 1994. Chem. Biol. 1 (4), 223–229.
Burris, K.P., Stewart, C.N., 2012. Trends Food Sci. Technol. 28 (2), 143–152.
Cao, J., Zhou, S., Kong, W., Yang, M., Wan, L., Yang, S., 2013. Food Control 33 (2), 337–343.
Cha, C., Shin, S.R., Annabi, N., Dokmeci, M.R., Khademhosseini, A., 2013. ACS Nano 7 (4), 2891–2897.
Chauhan, R., Singh, J., Sachdev, T., Basu, T., Malhotra, B.D., 2016. Biosens. Bioelectron. 81, 532–545.
Chen, J., Zhang, X., Cai, S., Wu, D., Chen, M., Wang, S., Zhang, J., 2014. Biosens. Bioelectron. 57, 226–231.
Cheng, C.I., Chang, Y.P., Chu, Y.H., 2012. Chem. Soc. Rev. 41 (5), 1947–1971.
Cheng, L., Qu, H., Teng, J., Yao, L., Xue, F., Chen, W., 2017. Food Science and Human Wellness 6 (2), 70–76.
Cho, E.J., Lee, J.W., Ellington, A.D., 2009. Annu. Rev. Anal. Chem. 2, 241–264.
Chu, X., Dou, X., Liang, R., Li, M., Kong, W., Yang, X., Luo, J., Yang, M., Zhao, M., 2016. Nanoscale 8 (7), 4127–4133.
Cieplak, M., Kutner, W., 2016. Trends Biotechnol. 34 (11), 922–941.
Cimpoca, G., Radulescu, C., I.V, P., Dulama, I., Bancuta, I., Gheboianu, A.,M.,C., Ileana, C.L.S., 2009. AIP Conference Proceedings 1203 (1), 415–420.
Cruz-Aguado, J.A., Penner, G., 2008. J. Agric. Food Chem. 56 (22), 10456–10461.
De Groof, T.W.M., Bobkov, V., Heukers, R., Smit, M.J., 2019. Mol. Cell. Endocrinol. 484, 15–24.
de Marco, A., 2011. Microb. Cell Factories 1 0, 44.
De Meyer, T., Muyldermans, S., Depicker, A., 2014. Trends Biotechnol. 32 (5), 263–270.
Dinshaw, I., Muniandy, S., Jyan Teh, S., Ibrahim, F., Leo, B., Thong, K.L., 2017. J. Electroanal. Chem. 806, 88–96.
Doria, G., Conde, J., Veigas, B., Giestas, L., Almeida, C., Assunção, M., Rosa, J., Baptista, P.V., 2012. Sensors 12 (2), 1657–1687.
El Khoury, A., Atoui, A., 2010. Toxins 2 (4), 461–493.
Ertekin, Ö., Öztürk, S., Öztürk, Z.Z., 2016. Sensors 16 (8).
Feng, J., Li, Y., Gao, Z., Lv, H., Zhang, X., Fan, D., Wei, Q., 2018. Biosens. Bioelectron. 99, 14–20.
Fernández-Baldo, M.A., Bertolino, F.A., Messina, G.A., Sanz, M.I., Raba, J., 2010. Talanta 83 (2), 651–657.
Fernández-Cruz, M.L., Mansilla, M.L., Tadeo, J.L., 2010. J. Adv. Res. 1 (2), 113–122.
Filip, J., Tkac, J., 2014. Electrochim. Acta 136, 340–354.
Ganbold, E.-O., Lee, C.M., Cho, E.-M., Son, S.J., Kim, S., Joo, S.-W., Yang, S.I., 2014. Anal. Methods-Uk 6 (11), 3573–3577.
Ge, X., Liu, J., Sun, L., 2017. Dalton Trans. 46 (48), 16729–16737.
George, J.M., Antony, A., Mathew, B., 2018. Microchim. Acta 185 (7), 358.
Gill, R., Zayats, M., Willner, I., 2008. Angew. Chem. Int. Ed. 47 (40), 7602–7625.
Giraudi, G., Ferrero, V.E.V., Anfossi, L., Baggiani, C., Giovannoli, C., Tozzi, C., 2015. J. Chromatogr. A 1422, 350.
Goud, K.Y., Kailasa, S.K., Kumar, V., Tsang, Y.F., Lee, S.E., Gobi, K.V., Kim, K.H., 2018. Biosens. Bioelectron. 121, 205–222.
Groff, K., Brown, J., Clippinger, A.J., 2015. Biotechnol. Adv. 33 (8), 1787–1798.
Gu, Y., Yan, X., Li, C., Zheng, B., Li, Y., Liu, W., Zhang, Z., Yang, M., 2016. Biosens. Bioelectron. 77, 393–399.
Gui, R., Jin, H., Guo, H., Wang, Z., 2018. Biosens. Bioelectron. 100, 56–70.
Guo, Z., Ren, J., Wang, J., Wang, E., 2011. Talanta 85 (5), 2517–2521.
Gupta, P.K., Tiwari, S., Khan, Z.H., Solanki, P.R., 2017. J. Mater. Chem. B 5 (10), 2019–2033.
Ha, T.H., 2015. Toxins (Basel) 7 (12), 5276–5300.
Hao, N., Jiang, L., Qian, J., Wang, K., 2016. J. Electroanal. Chem. 781, 332–338.
Hayat, A., Mishra, R.K., Catanante, G., Marty, J.L., 2015. Anal. Bioanal. Chem. 407 (25), 7815–7822.
He, Z.Y., He, Q., xu, Y., Li, Y.P., Liu, X., Chen, B., Lei, D., Sun, C.H., 2013. Anal. Chem. 85 (21), 10304–10311.
He, Y., Tian, F., Zhou, J., Jiao, B., 2019. Microchim. Acta 186, 199.
Hermann, T., Patel, D.J., 2000. Science 287 (5454), 820–825.
Holliger, P., Hudson, P.J., 2005. Nat. Biotechnol. 23 (9), 1126–1136.
Holthoff, E.L., Bright, F.V., 2007. Anal. Chim. Acta 594 (2), 147–161.
Hou, S.I., Ma, Z.E., Meng, H., Xu, Y., He, Q.H., 2018. Talanta 194, 919–924.
Hu, S., Ouyang, W., Guo, L., Lin, Z., Jiang, X., Qiu, B., Chen, G., 2017. Biosens. Bioelectron. 92, 718–723.
Huang, K.J., Shuai, H.L., Chen, Y.X., 2016. Sensor. Actuator. B Chem. 225, 391–397.
Huang, B., Xiao, L., Dong, H., Zhang, X., Gan, W., Mahboob, S., Al-Ghanim, K.A., Yuan, Q., Li, Y., 2017. Talanta 164, 601–607.
Hun, X., Liu, F., Mei, Z., Ma, L., Wang, Z., Luo, X., 2013. Biosens. Bioelectron. 39 (1), 145–151.
Hung, Y.L., Hsiung, T.M., Chen, Y.Y., Huang, Y.F., Huang, C.C., 2010. J. Phys. Chem. C 114 (39), 16329–16334.
Iqbal, S.Z., Asi, M.R., Hanif, U., Zuber, M., Jinap, S., 2016. Food Chem. 210, 135–140.
Jalalvand, A.R., 2018. Talanta 188, 225–231.
Jeong, Y., Kook, Y.M., Lee, K., Koh, W.G., 2018. Biosens. Bioelectron. 111, 102–116.
Jiang, L., Qian, J., Yang, X., Yan, Y., Liu, Q., Wang, K., Wang, K., 2014. Anal. Chim. Acta 806, 128–135.
Jiang, H., Li, X., Xiong, Y., Pei, K., Nie, L., Xiong, Y., 2017. Toxins 9 (3).
Jiang, C., Lan, L., Yao, Y., Zhao, F., Ping, J., 2018. Trac. Trends Anal. Chem. 102, 236–249.
Jo, E.J., Mun, H., Kim, S.J., Shim, W.B., Kim, M.G., 2016. Food Chem. 194, 1102–1107.
Kaittanis, C., Santra, S., Perez, J.M., 2010. Adv. Drug Deliv. Rev. 62 (4–5), 408–423.
Karczmarczyk, A., Reiner-Rozman, C., Hageneder, S., Dubiak-Szepietowska, M., Dostalek, J., Feller, K.H., 2016. Anal. Chim. Acta 937, 143–150.
Karczmarczyk, A., Baeumner, A.J., Feller, K.-H., 2017a. Electrochim. Acta 243, 82–89.
Karczmarczyk, A., Haupt, K., Feller, K.H., 2017b. Talanta 166, 193–197.
Karimi, A., Hayat, A., Andreescu, S., 2017. Biosens. Bioelectron. 87, 501–507.
Kaur, N., Bharti, A., Batra, S., Rana, S., Rana, S., Bhalla, A., Prabhakar, N., 2019. Microchem. J. 144, 102–109.
Könning, D., Zielonka, S., Grzeschik, J., Empting, M., Valldorf, B., Krah, S., Schröter, C., Sellmann, C., Hock, B., Kolmar, H., 2017. Curr. Opin. Struct. Biol. 45, 10–16.
Kuila, T., Bose, S., Khanra, P., Mishra, A.K., Kim, N.H., Lee, J.H., 2011. Biosens. Bioelectron. 26 (12), 4637–4648.
Lai, X., Ruan, C., Liu, R., Liu, C., 2014. Food Chem. 161, 317–322.
Lawal, A.T., 2018. Biosens. Bioelectron 106, 149–178.
Lee, B., Park, J.H., Byun, J.Y., Kim, J.H., Kim, M.G., 2018. Biosens. Bioelectron. 102, 504–509.
Li, Y., Chen, Q., Xu, X., Jin, Y., Wang, Y., Zhang, L., Yang, W., He, L., Feng, X., Chen, Y., 2018. Sensor. Actuator. B Chem. 266, 115–123.
Liang, Y., Huang, X., Yu, R., Zhou, Y., Xiong, Y., 2016. Anal. Chim. Acta 936, 195–201.
Lin, C., Zheng, H., Sun, M., Guo, Y., Luo, F., Guo, L., Qiu, B., Lin, Z., Chen, G., 2018. Anal. Chim. Acta 1002, 90–96.
Liu, X., Xu, Y., Xiong, Y.H., Tu, Z., Li, Y.P., He, Z.Y., Qiu, Y.L., Fu, J.H., Gee, S.J., Hammock, B.D., 2014. Anal. Chem. 86 (15), 7471–7477.
Liu, Q., Wang, J., Boyd, B.J., 2015. Talanta 136, 114–127.
Liu, W., Ma, Y., Sun, G., Wang, S., Deng, J., Wei, H., 2017a. Biosens. Bioelectron. 92, 305–312.
Liu, X., Tang, Z., Duan, Z., He, Z., Shu, M., Wang, X., Gee, S.J., Hammock, B.D., Xu, Y., 2017b. Talanta 164, 154–158.
Loo, A.H., Bonanni, A., Pumera, M., 2015. ChemElectroChem 2 (5), 743–747.
Lu, L., Seenivasan, R., Wang, Y.C., Yu, J.H., Gunasekaran, S., 2016. Electrochim. Acta 213, 89–97.
Lu, Z., Chen, X., Hu, W., 2017. Sensor. Actuator. B Chem. 246, 61–67.
Luan, Y., Chen, J., Li, C., Xie, G., Fu, H., Ma, Z., Lu, A., 2015. Toxins 7 (12).
Lv, L., Cui, C., Liang, C., Quan, W., Wang, S., Guo, Z., 2016. Food Control 60, 296–301.
Lv, L., Li, D., Cui, C., Zhao, Y., Guo, Z., 2017a. Biosens. Bioelectron. 87, 136–141.
Lv, L., Li, D., Liu, R., Cui, C., Guo, Z., 2017b. Sensor. Actuator. B Chem. 246, 647–652.
Lv, X., Zhang, Y., Liu, G., Du, L., Wang, S., 2017c. RSC Adv. 7 (27), 16290–16294.
Lv, L., Jin, Y., Kang, X., Zhao, Y., Cui, C., Guo, Z., 2018. Food Chem. 249, 45–50.
Ma, C., Liu, H., Tian, T., Song, X., Yu, J., Yan, M., 2016. Biosens. Bioelectron. 83, 15–18.
Ma, Y., Shen, X.L., Zeng, Q., Wang, H.S., Wang, L.S., 2017. Talanta 164, 121–127.
Mahdi, M., Mansour, B., Afshin, M., 2016. Microchim. Acta 183 (12), 3093–3099.
Mahdiannasser, M., Karami, Z., 2018. Biosens. Bioelectron. 107, 123–144.
Mahmoudpour, M., Ezzati Nazhad Dolatabadi, J., Torbati, M., Homayouni-Rad, A., 2019. Biosens. Bioelectron. 127, 72–84.
Majdinasab, M., Sheikh-Zeinoddin, M., Soleimanian-Zad, S., Li, P., Zhang, Q., Li, X., Tang, X., 2015. J. Chromatogr. B 974, 147–154.
Malvano, F., Albanese, D., Crescitelli, A., Pilloton, R., Esposito, E., 2016a. Biosensors 6 (3), 33.
Malvano, F., Albanese, D., Pilloton, R., Di Matteo, M., 2016b. Food Chem. 212, 688–694.

Mariño-Repizo, L., Kero, F., Vandell, V., Senior, A., Isabel Sanz-Ferramola, M., Cerutti, S., Raba, J., 2015. Food Chem. 172, 663–668.
Marx, K.A., 2003. Biomacromolecules 4 (5), 1099–1120.
Masdor, N.A., Altintas, Z., Tothill, I.E., 2016. Biosens. Bioelectron. 78, 328–336.
Meulenberg, E.P., 2012. Toxins 4 (4), 244–266.
Mishra, R.K., Hayat, A., Catanante, G., Istamboulie, G., Marty, J.L., 2016. Food Chem. 192, 799–804.
Mishra, K.G., Sharma, V., Mishra, K.R., 2018. Biosensors 8 (2), 35.
Mohammadzadeh-Asl, S., Keshtkar, A., Ezzati Nazhad Dolatabadi, J., de la Guardia, M., 2018. Biosens. Bioelectron. 110, 118–131.
Mondal, S., Rana, U., Malik, S., 2015. Chem. Commun. 51 (62), 12365–12368.
Mun, H., Jo, E.-J., Li, T., Joung, H.A., Hong, D.G., Shim, W.B., Jung, C., Kim, M.G., 2014. Biosens. Bioelectron. 58, 308–313.
Mutlu, S., 2010. Mass Sensitive Biosensors. pp. 71–87.
Muyldermans, S., 2013. Annu. Rev. Biochem. 82, 775–797.
Nath, S., Kaittanis, C., Tinkham, A., Perez, J.M., 2008. Anal. Chem. 80 (4), 1033–1038.
Niazi, S., Wang, X., Pasha, I., Khan, I.M., Zhao, S., Shoaib, M., Wu, S., Wang, Z., 2018. Talanta 186, 97–103.
Norouzi, P., Alahdadi, I., Shahtaheri, S., 2015. Int. J. Electrochem. Sci. 10 (4), 3400–3413.
Novo, P., Moulas, G., França Prazeres, D.M., Chu, V., Conde, J.P., 2013. Sensor. Actuator. B Chem. 176, 232–240.
Olsson, J., Börjesson, T., Lundstedt, T., Schnürer, J., 2002. Int. J. Food Microbiol. 72 (3), 203–214.
Pacheco, J.G., Castro, M., Machado, S., Barroso, M.F., Nouws, H.P.A., Delerue-Matos, C., 2015. Sensor. Actuator. B Chem. 215, 107–112.
Park, J.H., Byun, J.Y., Mun, H., Shim, W.B., Shin, Y.B., Li, T., Kim, M.G., 2014. Biosens. Bioelectron. 59, 321–327.
Pei, K., Xiong, Y., Xu, B., Wu, K., Li, X., Jiang, H., Xiong, Y., 2018. Sensor. Actuator. B Chem. 262, 102–109.
Pfeiffer, F., Mayer, G., 2016. Front. Chem. 4, 25.
Piletsky, S.A., Turner, N.W., Laitenberger, P., 2006. Med. Eng. Phys. 28 (10), 971–977.
Poma, A., Turner, A.P.F., Piletsky, S.A., 2010. Trends Biotechnol. 28 (12), 629–637.
Qian, J., Jiang, L., Yang, X., Yan, Y., Mao, H., Wang, K., 2014. Analyst 139 (21), 5587–5593.
Qian, J., Wang, K., Wang, C., Hua, M., Yang, Z., Liu, Q., Mao, H., Wang, K., 2015. Analyst 140 (21), 7434–7442.
Qian, J., Ren, C., Wang, C., Chen, W., Lu, X., Li, H., Liu, Q., Hao, N., Li, H., Wang, K., 2018. Anal. Chim. Acta 1019, 119–127.
Qileng, A., Wei, J., Lu, N., Liu, W., Cai, Y., Chen, M., Lei, H., Liu, Y., 2018. Biosens. Bioelectron. 106, 219–226.
Qiu, Q., Chen, H., Wang, Y., Ying, Y., 2019. Coord. Chem. Rev. 387, 60–78.
Rai, M., Jogee, P., Ingle, A., 2015. Int. J. Food Sci. Nutr. 66 (4), 363–370.
Ratautaite, V., Plausinaitis, D., Baleviciute, I., Mikoliunaite, L., Ramanaviciene, A., Ramanavicius, A., 2015. Sensor. Actuator. B Chem. 212, 63–71.
Regiart, M., Fernández, O., Vicario, A., Villarroel-Rocha, J., Sapag, K., Messina, G.A., Raba, J., Bertolino, F.A., 2018. Microchem. J. 141, 388–394.
Rehmat, Z., Mohammed, W.S., Sadiq, M.B., Somarapalli, M., Kumar Anal, A., 2019. Colloids Surf., B 174, 569–574.
Ren, C., Li, H., Lu, X., Qian, J., Zhu, M., Chen, W., Liu, Q., Hao, N., Li, H., Wang, K., 2017. Sensor. Actuator. B Chem. 251, 192–199.
Ren, X., Lu, P., Feng, R., Zhang, T., Zhang, Y., Wu, D., Wei, Q., 2018. Talanta 188, 593–599.
Ribes, À., Santiago-Felipe, S., Bernardos, A., Marcos, M.D., Pardo, T., Sancenón, F., Martínez-Máñez, R., Aznar, E., 2017. ChemistryOpen 6 (5), 653–659.
Rivas, L., Mayorga-Martinez, C.C., Quesada-Gonzalez, D., Zamora-Galvez, A., de la Escosura-Muniz, A., Merkoci, A., 2015. Anal. Chem. 87 (10), 5167–5172.
Rowley-Neale, S.J., Randviir, E.P., Abo Dena, A.S., Banks, C.E., 2018. Appl. Mater.Today 10, 218–226.
Savastano, M.L., Losito, I., Pati, S., 2016. Food Control 68, 391–398.
Shanshan Wang, X.Z.a.M.Z., 2012. Optical Sensors Based on Molecularly Imprinted Nanomaterials. Bentham, Oak Park, pp. 60–75.
Shao, B., Ma, X., Zhao, S., Lv, Y., Hun, X., Wang, H., Wang, Z., 2018. Anal. Chim. Acta 1033, 165–172.
Sharma, A., Hayat, A., Mishra, R.K., Catanante, G., Bhand, S., Marty, J.L., 2015. Toxins 7 (9), 3771–3784.
Shen, P., Li, W., Liu, Y., Ding, Z., Deng, Y., Zhu, X., Jin, Y., Li, Y., Li, J., Zheng, T., 2017. Anal. Chem. 89 (21), 11862–11868.
Shen, P., Li, W., Ding, Z., Deng, Y., Liu, Y., Zhu, X., Cai, T., Li, J., Zheng, T., 2018. Anal. Biochem. 554, 28–33.
Shi, L., Rong, X., Wang, Y., Ding, S., Tang, W., 2018. Biosens. Bioelectron. 102, 41–48.
Shu, J., Tang, D., 2017. Chemistry – An Asian Journal 12 (21), 2780–2789.
Silva, B.V.M., Rodríguez, B.A.G., Sales, G.F., Sotomayor, M.D.P.T., Dutra, R.F., 2016. Biosens. Bioelectron. 77, 978–985.
Solanki, P.R., Singh, J., Rupavali, B., Tiwari, S., Malhotra, B.D., 2017. Mat. Sci. Eng C-Mater. 70, 564–571.
Soleri, R., Demey, H., Tria, S.A., Guiseppi-Elie, A., Ibn Had Hassine, A., Gonzalez, C., Bazin, I., 2015. Biosens. Bioelectron. 67, 634–641.
Song, D., Yang, R., Fang, S., Liu, Y., Long, F., Zhu, A., 2018. Microchim. Acta 185 (10), 491.
Steeland, S., Vandenbroucke, R.E., Libert, C., 2016. Drug Discov. Today 21 (7), 1076–1113.
Sun, A.L., Zhang, Y.F., Sun, G.P., Wang, X.N., Tang, D., 2017. Biosens. Bioelectron. 89, 659–665.
Sun, Z., Wang, X., Tang, Z., Chen, Q., Liu, X., 2019. Ecotoxicol. Environ. Saf. 171, 382–388.
Taghdisi, S.M., Danesh, N.M., Beheshti, H.R., Ramezani, M., Abnous, K., 2016. Nanoscale 8 (6), 3439–3446.
Tan, Y., Wei, X., Zhang, Y., Wang, P., Qiu, B., Guo, L., Lin, Z., Yang, H.H., 2015. Anal. Chem. 87 (23), 11826–11831.
Tang, J., Huang, Y., Zhang, C., Liu, H., Tang, D., 2016. Biosens. Bioelectron. 86, 386–392.
Tang, M.S.L., Shiu, S.C.-C., Godonoga, M., Cheung, Y.-W., Liang, S., Dirkzwager, R.M., Kinghorn, A.B., Fraser, L.A., Heddle, J.G., Tanner, J.A., 2018a. Nanomed. Nanotechnol. 14 (4), 1161–1168.
Tang, Z., Wang, X., Lv, J., Hu, X., Liu, X., 2018b. Food Control 92, 430–436.
Teixeira, T.R., Hoeltz, M., Einloft, T., Dottori, H., Manfroi, V., Noll, I.B., 2011. Food Addit. Contam. B 4 (4), 289–293.
Terra, I.A.A., Mercante, L.A., Andre, R.S., Correa, D.S., 2017. Biosensors 7 (4).
Tian, J., Wei, W., Wang, J., Ji, S., Chen, G., Lu, J., 2018. Anal. Chim. Acta 1000, 265–272.
Tong, P., Zhao, W.-W., Zhang, L., Xu, J.-J., Chen, H.-Y., 2012. Biosens. Bioelectron. 33 (1), 146–151.
Tozzi, C., Anfossi, L., Giraudi, G., Giovannoli, C., Baggiani, C., Vanni, A., 2002. J. Chromatogr. A 966 (1–2), 71–79.
Tria, S.A., Lopez-Ferber, D., Gonzalez, C., Bazin, I., Guiseppi-Elie, A., 2016. Biosens. Bioelectron. 79, 835–842.
Turan, E., Şahin, F., 2016. Sensor. Actuator. B Chem. 227, 668–676.
Turner, N.W., Bramhmbhatt, H., Szabo-Vezse, M., Poma, A., Coker, R., Piletsky, S.A., 2015. Anal. Chim. Acta 901, 12–33.
Van Audenhove, I., Gettemans, J., 2016. Ebiomedicine 8, 40–48.
van Egmond, H.P., Schothorst, R.C., Jonker, M.A., 2007. Anal. Bioanal. Chem. 389 (1), 147–157.
Van Heeke, G., Allosery, K., De Brabandere, V., De Smedt, T., Detalle, L., de Fougerolles, A., 2017. Pharmacol Ther 169, 47–56.
Velusamy, V., Arshak, K., Korostynska, O., Oliwa, K., Adley, C., 2010. Biotechnol. Adv. 28 (2), 232–254.
Wang, Z., Duan, N., Hun, X., Wu, S., 2010. Anal. Bioanal. Chem. 398 (5), 2125–2132.
Wang, C., Dong, X., Liu, Q., Wang, K., 2015a. Anal. Chim. Acta 860, 83–88.
Wang, C., Qian, J., Wang, K., Wang, K., Liu, Q., Dong, X., Wang, C., Huang, X., 2015b. Biosens. Bioelectron. 68, 783–790.
Wang, K., Gan, L., Jiang, L., Zhang, X., Yang, X., Chen, M., Lan, X., 2015c. Antimicrob. Agents. Ch 59 (4), 2072.
Wang, B., Wu, Y., Chen, Y., Weng, B., Xu, L., Li, C., 2016a. Biosens. Bioelectron. 81, 125–130.
Wang, C., Qian, J., Wang, K., Yang, X., Liu, Q., Hao, N., Wang, C., Dong, X., Huang, X., 2016b. Biosens. Bioelectron. 77, 1183–1191.
Wang, D., Wang, Z., Chen, J., Kinchla, A.J., Nugen, S.R., 2016c. Food Control 62, 81–88.
Wang, Q., Chen, M., Zhang, H., Wen, W., Zhang, X., Wang, S., 2016d. Biosens. Bioelectron. 79, 561–567.
Wang, Q., Chen, M., Zhang, H., Wen, W., Zhang, X., Wang, S., 2016e. Sensor. Actuator. B Chem. 222, 264–269.
Wang, Z., Yu, J., Gui, R., Jin, H., Xia, Y., 2016f. Biosens. Bioelectron. 79, 136–149.
Wang, K., He, M.Q., Zhai, F.H., He, R.H., Yu, Y.L., 2017a. Talanta 166, 87–92.
Wang, R., Wang, L., Callaway, Z.T., Lu, H., Huang, T.J., Li, Y., 2017b. Sensor. Actuator. B Chem. 240, 934–940.
Wang, S., Zhang, Y., Pang, G., Zhang, Y., Guo, S., 2017c. Anal. Chem. 89 (3), 1704–1709.
Wang, T., Zhou, Y., Lei, C., Luo, J., Xie, S., Pu, H., 2017d. Biosens. Bioelectron. 90, 418–435.
Wang, Z., Yu, H., Han, J., Xie, G., Chen, S., 2017e. Chem. Commun. 53 (71), 9926–9929.
Wang, C., Tan, R., Chen, D., 2018a. Talanta 182, 363–370.
Wang, G., Morrin, A., Li, M., Liu, N., Luo, X., 2018b. J. Mater. Chem. B 6 (25), 4173–4190.
Wei, M., Feng, S., 2017. Anal. Methods-Uk 9 (37), 5449–5454.
Wei, M., Zhang, W., 2017. RSC Adv. 7 (46), 28655–28660.
Wei, Y., Zhang, J., Wang, X., Duan, Y., 2015. Biosens. Bioelectron. 65, 16–22.
Willander, M., Khun, K., Ibupoto, Z.H., 2014. Sensors 14 (5), 8605–8632.
Witt, M., Walter, J.-G., Stahl, F., 2015. Microarrays 4 (2).
Wu, Y., Jiang, T., Wu, Z., Yu, R., 2018a. Talanta 185, 30–36.
Wu, S., Liu, L., Duan, N., Wang, W., Yu, Q., Wang, Z., 2018b. Microchim. Acta 185 (11), 497.
Wu, L., Li, G., Xu, X., Zhu, L., Huang, R., Chen, X., 2019. Trac. Trends Anal. Chem. 113, 140–156.
Xiao, R., Wang, D., Lin, Z., Qiu, B., Liu, M., Guo, L., Chen, G., 2015. Anal. Methods-Uk 7 (3), 842–845.
Xiao, M.-W., Bai, X.-L., Liu, Y.-M., Yang, L., Liao, X., 2018. J. Chromatogr. A 1569, 222–228.
Xie, S., Chai, Y., Yuan, Y., Bai, L., Yuan, R., 2014. Biosens. Bioelectron. 55, 324–329.
Xu, X., Xu, C., Ying, Y., 2016. RSC Adv. 6 (56), 50437–50443.
Yan, S., Fang, Y., Gao, Z., 2007. Biosens. Bioelectron. 22 (6), 1087–1091.
Yang, C., Lates, V., Prieto-Simón, B., Marty, J.L., Yang, X., 2013. Talanta 116, 520–526.
Yang, M., Jiang, B., Xie, J., Xiang, Y., Yuan, R., Chai, Y., 2014a. Talanta 125, 45–50.
Yang, X., Qian, J., Jiang, L., Yan, Y., Wang, K., Liu, Q., Wang, K., 2014b. Bioelectrochemistry 96, 7–13.
Yang, J., Gao, P., Liu, Y., Li, R., Ma, H., Du, B., Wei, Q., 2015a. Biosens. Bioelectron. 64, 13–18.
Yang, L., Zhang, Y., Li, R., Lin, C., Guo, L., Qiu, B., Lin, Z., Chen, G., 2015b. Biosens. Bioelectron. 70, 268–274.
Yang, Y., Li, W., Shen, P., Liu, R., Li, Y., Xu, J., Zheng, Q., Zhang, Y., Li, J., Zheng, T., 2017. Sensor. Actuator. B Chem. 248, 351–358.
Yao, L., Chen, Y., Teng, J., Zheng, W., Wu, J., Adeloju, S.B., Pan, D., Chen, W., 2015. Biosens. Bioelectron. 74, 534–538.
Yao, J., Xing, G., Han, J., Sun, Y., Wang, F., Deng, R., Hu, X., Zhang, G., 2017. J. Biophot. 10 (5), 657–663.

Yazdian robati, R., Arab, A., Ramezani, M., Abnous, K., Taghdisi, S.M., 2016. Biosens. Bioelectron. 82, 162–172.
Yim, S.Y., Park, J.H., Kim, M.G., 2015. International Conference on Nano-Bio Sensing, Imaging, and Spectroscopy 2015. SPIE, pp. 5.
Yin, X., Wang, S., Liu, X., He, C., Tang, Y., Li, Q., Liu, J., Su, H., Tan, T., Dong, Y., 2017. Anal. Sci. 33 (6), 659–664.
Yola, M.L., Gupta, V.K., Atar, N., 2016. Mat. Sci. Eng. C-Mater. 61, 368–375.
You, M., Yang, S., Tang, W., Zhang, F., He, P., 2018. Biosens. Bioelectron. 112, 72–78.
Yu, S., He, L., Yu, F., Liu, L., Qu, C., Qu, L., Liu, J., Wu, Y., Wu, Y., 2018a. Toxicon 156, 23–27.
Yu, X., Chen, F., Wang, R., Li, Y., 2018b. J. Biotechnol. 266, 39–49.
Yu, X.H., Lin, Y.H., Wang, X.S., Xu, L.J., Wang, Z.W., Fu, F.F., 2018c. Microchim. Acta 185, 259.
Yuan, Y., Wei, S., Liu, G., Xie, S., Yaqin, C., Yuan, R., 2014. Anal. Chim. Acta 811, 70–75.
Yuan, H., Huang, Y., Yang, J., Guo, Y., Zeng, X., Zhou, S., Cheng, J., Zhang, Y., 2018. Spectrochim. Acta, A 200, 330–338.
Zamora-Gálvez, A., Morales-Narváez, E., Mayorga-Martinez, C.C., Merkoçi, A., 2017. Appl. Mater. Today 9, 387–401.
Zhang, A., Ma, Y., Feng, L., Wang, Y., He, C., Wang, X., Zhang, H., 2011. Food Control 22 (11), 1723–1728.
Zhang, Y., Qi, X., Zheng, J., Luo, Y., Zhao, C., Hao, J., Li, X., Huang, K., Xu, W., 2015. J. Biochem. Mol. Toxicol. 30 (2), 71–79.
Zhang, J., Xia, Y.K., Chen, M., Wu, D.Z., Cai, S.X., Liu, M.M., He, W.H., Chen, J.H., 2016a. Sensor. Actuator. B Chem. 235, 79–85.
Zhang, X., Li, C.R., Wang, W.C., Xue, J., Huang, Y.L., Yang, X.X., Tan, B., Zhou, X.P., Shao, C., Ding, S.J., Qiu, J.F., 2016b. Food Chem. 192, 197–202.
Zhang, G., Zhu, C., Huang, Y., Yan, J., Chen, A., 2018. Molecules 23 (2), 291.
Zhao, X., Yuan, Y., Zhang, X., Yue, T., 2014. Food Control 46, 332–337.
Zhao, X.H., Meng, H.M., Gong, L., Qiu, L.P., Zhang, X.B., Tan, W.H., 2015a. Chin. J. Anal. Chem. 43 (11), 1611–1619.
Zhao, Y., Yang, Y., Luo, Y., Yang, X., Li, M., Song, Q., 2015b. Acs. Appl. Mater. Inter. 7 (39), 21780–21786.
Zhao, W.W., Yu, X.D., Xu, J.J., Chen, H.Y., 2016. Nanoscale 8 (40), 17407–17414.
Zhao, Y., Liu, R., Sun, W., Lv, L., Guo, Z., 2018. Sensor. Actuator. B Chem. 255, 1640–1645.
Zhu, Z., Feng, M., Zuo, L., Zhu, Z., Wang, F., Chen, L., Li, J., Shan, G., Luo, S.Z., 2015. Biosens. Bioelectron. 65, 320–326.
Zhu, W., Ren, C., Nie, Y., Xu, Y., 2016. Food Control 64, 37–44.
Zhu, X., Kou, F., Xu, H., Han, Y., Yang, G., Huang, X., Chen, W., Chi, Y., Lin, Z., 2018. Sensor. Actuator. B Chem. 270, 263–269.
Zinedine, A., Blesa, J., Mahnine, N., El Abidi, A., Montesano, D., Mañes, J., 2010. Food Control 21 (2), 132–135.
Zou, X., Chen, C., Huang, X., Chen, X., Wang, L., Xiong, Y., 2016. Talanta 146, 394–400.